

## **Exploration of a Viral Protein for Cancer Therapy**

Victoria Carter, McKenzie Funk, Jordan Johnson, Dominic Lanasa, Eva Loewenstein, Katherine Luo, Grishma Patel, Eileen Shih, Rotimi Sofola, Sruthi Srinivasan

Apr 30, 2023

Team E.V. I.C.T.

Enacting a Viral Protein in Cancer Therapy

Gemstone Honors Program, University of Maryland, College Park, MD

Mentor: Dr. Yanjin Zhang

Librarian: Nedelina Tchangalova

### **Acknowledgements**

We would like to thank our mentor Dr. Yanjin Zhang, for his continued support and guidance.

We are thankful for the assistance from members of the Zhang Lab, namely Mr. Bhargava Teja Sallapalli and Ms. Peixi Chang. We thank Ms. Nedelina Tchangalova for her guidance as our team librarian. We acknowledge funding support from generous donors at LaunchUMD, the Do Good Institute, and UMD Libraries for our project. We are grateful to the Gemstone Honors Program—Dr. David Lovell, Dr. Kristan Skendall, Dr. Allison Lansverk, Dr. Leah Tobin, Dr. Vickie Hill, Ms. Jessica Lee, and Ms. Jalah Townsend—for the opportunity to engage in extensive, interdisciplinary research as undergraduate students. Finally, we appreciate our discussants for reviewing our thesis and providing feedback and the team members' family and friends for their continuous support.

## Table of Contents

<b>Abstract</b>	<b>6</b>
<b>Chapter 1. Introduction</b>	<b>7</b>
Research Question and Objectives	8
<b>Chapter 2. Literature Review</b>	<b>8</b>
Overview of Cancer	8
Overview of Lymphoma	9
Overview of STAT3	10
Structure of STAT3	11
STAT3 in Cancer	14
Mechanism of STAT3 Signaling and Cancer Development	15
Development of STAT3 Inhibitors for Cancer Treatment	20
Overview of nsp5	24
Expression of nsp5	24
Effects of nsp5 protein on STAT3	26
Gene Delivery	28
<b>Chapter 3. Methodology</b>	<b>31</b>
Plasmid Construction	31
Transfection of GP2-293 cells	33
Reverse transcription and real-time PCR (RT-qPCR)	34
Transduction of lymphoma cell line by retroviral particles	34
Western Blot Analysis	35
<b>Chapter 4. Results</b>	<b>37</b>
Cloning of nsp5-D4 into pLNCX2-VenusC1	37
Optimization of Retroviral Packaging	39
Retrovirus Titration	43
Transduction	46
Western Blotting Detection of STAT3	48
<b>Chapter 5. Discussion</b>	<b>52</b>
Cloning of nsp5-D4 into pLNCX2-VenusC1	52
Optimization of Retroviral Packaging	53
Retroviral Titration	54
Transduction	55
Western Blotting Detection of STAT3	56
Cell Viability Assay	56
Limitations	57
Relevance	58

Future Directions	59
<b>Chapter 6. Conclusions</b>	<b>60</b>
<b>References</b>	<b>62</b>
<b>Appendices</b>	<b>80</b>
Appendix A: PCR Amplification of Target Genes and Cloning	80
A.1 D4 Amplification	80
A.2 Purification of PCR product (Using GeneJET PCR purification kit)	82
A.3 Checking DNA Concentration (using BioTek software)	83
A.4 Sanger Sequencing	84
A.5 Double-Restriction Enzyme Digestion	87
A.6 Ligation	89
A.7 Colony PCR	91
A.8 Running DNA Gel (Using Quality One App for analysis)	92
A.9 Miniprep	94
A.9.1 Inoculation for Miniprep	94
A.9.2 Running Miniprep (Using GeneJET PCR purification kit)	94
A.10 Midiprep	96
A.10.1 Inoculation for Midiprep	96
A.10.2 Running Midiprep (PureYield Plasmid Midiprep System)	96
Appendix B: Retroviral Packaging and Delivery through Transfection	99
B.1 Recombinant Plasmid	99
B.2 Packaging Retroviral Vectors	99
B.3 Harvesting the Retroviruses from GP2-293 cells	100
B.4 Determining Retroviral Titer by qRT-PCR	101
B.4.1 Protocol Overview	102
B.4.2 Purifying Retroviral Genomic RNA	102
B.4.3 qRT-PCR amplification (PCR room)	103
Appendix C: Transduction of target gene into Lymphoma cell line	108
C.1 Delivery of packaged retroviruses into BCBL-1 cell line	109
C.2 Harvesting BCBL-1 Cells for Analysis on Gene Expression	110
Appendix D: Cell Culture and Maintenance	111
D.1 Subculturing Mammalian Cells	111
D.1.1 GP2-293 Cells (Adherent)	111
D.1.2 BCBL-1 Cells (Suspension)	113
Appendix E: Equity Impact	114
Appendix E.1: Equity-Centered Design Model	116

### **Abstract**

Cancer is a group of malignant diseases and is one of the leading causes of death worldwide. Current treatments can be invasive and nonspecific, therefore killing healthy cells along with cancerous cells. In many types of cancers including lymphoma, signal transducer and activator of transcription 3 (STAT3) is upregulated and regarded as a risk factor for its enhancing tumorigenicity. Thus, STAT3 is a target for cancer therapy. In this project, we explored a viral protein called nsp5 that induces the degradation of STAT3 to develop cancer therapeutics against lymphoma. We cloned the nsp5 gene into a retroviral expression system and determined its expression. Replication-defective retrovirus particles were packaged and used to deliver nsp5 gene into the lymphoma-derived cells. The nsp5 effect on downregulation of STAT3 and tumor cell growth were determined. These results demonstrate that the viral protein can be explored for further preclinical development for potential tumor therapeutics.

*Keywords:* cancer, therapeutics, lymphoma, PRRSV, STAT3, nsp5, retrovirus

## Chapter 1. Introduction

Cancer is one of the most alarming and widespread diseases around the world, with nearly 10 million deaths each year and is one of the leading causes of death globally (World Health Organization, 2022). Among the many types of cancer, lymphoma is a tumor that arises from the cells in the lymphatic system and is one of the most common types of cancer (National Cancer Institute, 2022b; National Cancer Institute, 2022c; American Cancer Society, 2023). Current cancer treatments include chemotherapy, radiation, and surgery (National Cancer Institute, 2022b; National Cancer Institute, 2022c). While these treatments can be effective, they often have disadvantages. Surgery can be highly invasive while chemotherapy and radiation can impact normal functioning cells in the body and have significant negative side effects (Center for Disease Control and Prevention, 2022). Exploration of specific genes and signaling pathways that influence the development and progression of cancer for better targeted, more effective, and less toxic treatments has become a favored approach (Wang et al., 2020b). Since transcription factors regulate gene expression, targeting them for therapeutic treatment is explored to reduce oncogene expression and subsequent tumor development.

One well-studied transcription factor is the signal transducer and activator of transcription 3 (STAT3), which is involved in the Janus kinase (JAK)/STAT signaling pathway (Li et al., 2020; Zhu et al., 2019). STAT3 is a pleiotropic protein that is activated in response to various cytokines, growth factors, and oncogene signals (Bai et al., 2019; Bharadwaj et al., 2014, Son et al., 2017). STAT3 has been demonstrated to play an important role in many cellular processes including oncogenesis, tumor growth and progression, stemness, differentiation, and immune response (Arshad et al., 2020; Bai et al., 2019; Carpenter & Lo, 2014; Chai et al., 2016; Huang et al., 2014; Li et al., 2020; Lü et al., 2021). In a study done by L. Yang and colleagues

(Yang et al., 2017), the nonstructural protein 5 (nsp5) of Porcine Reproductive and Respiratory Syndrome Virus (PRRSV) was shown to downregulate STAT3.

### **Research Question and Objectives**

The research question of our team was: How can we optimize the nsp5 expression to downregulate STAT3 in lymphoma cells in order to induce cancer cell death?

The objective of this research was to explore nsp5 to inhibit proliferation of lymphoma cells by downregulating STAT3. To address this objective, we proposed to work on the following two aims: (1) to construct a retroviral delivery system to deliver nsp5 into lymphoma cells and (2) to analyze nsp5 effect on STAT3 expression and subsequent cell growth in a lymphoma cell line.

In this study, by employing molecular biology, we cloned and expressed nsp5 using the retrovirus delivery system to reduce STAT3 in lymphoma cells. The expression of nsp5 and STAT3 level in the target cells was determined. Lymphoma cell growth was monitored. Data from this research may facilitate future development of an effective and less toxic cancer therapy.

## **Chapter 2. Literature Review**

### **Overview of Cancer**

Cancer is characterized by the rapid and abnormal growth and spread of cells due to genetic changes that impact the life cycle and function of cells (National Cancer Institute, 2021). Such uncontrolled growth results in a multitude of biological and physiological issues that are detrimental to the health of an individual. There are five stages of cancer development (National Cancer Institute, 2022a). The stage numbers correspond to the size of tumors and the spread of

cancer cells to nearby tissues. The larger the tumor and the greater the spread, the higher the stage number. The first stage is known as stage zero, where there is a presence of abnormal cells, but they have not spread to nearby tissues. Stages I, II, and III refer to the presence of tumors and metastasis of nearby tissues. Stage IV refers to the presence of tumors and the metastasis of the cancer cells to distant tissues. A localized mass of abnormal cells becomes cancer when metastasis occurs (National Cancer Institute, 2021). Metastasis involves the spread of cancer cells to nearby and distant tissues and organs and is the primary cause of cancer mortality and morbidity (Seyfried & Huysentruyt, 2013).

Cancer is one of the leading causes of death worldwide (World Health Organization, 2022). Current treatment methods can be effective but exert significant side effects that include pain, fatigue, nausea and vomiting, hair loss, and cognitive problems (Centers for Disease Control and Prevention, 2022). Beyond the health impacts, cancer causes issues in numerous other domains. The long duration and high cost of treatment put a financial strain on patients, their families, and the healthcare system (National Cancer Institute, 2020; Mariotto et al., 2020).

## **Overview of Lymphoma**

There are more than one hundred different types of cancer with the symptoms ranging from fatigue and fever to unusual bleeding and organ dysfunction (National Cancer Institute, 2019). One such cancer is lymphoma, a tumor that arises from the cells in the lymphatic system (National Cancer Institute, 2022b; American Cancer Society, 2023). Lymphoma is one of the most common types of cancer with estimated new cases of 89,010 and deaths of 21,170 in 2022 in the United States (Siegel et al., 2022). There are two main types of lymphomas: Hodgkin and Non-Hodgkin (Wang et al., 2020b). Hodgkin's lymphoma is characterized by Reed-Sternberg cells that are abnormal and large B cells (National Cancer Institute, 2022b). Non-Hodgkin's

lymphoma includes the presence of abnormal B and T cells that can arise throughout the body (National Cancer Institute, 2022c). Non-Hodgkin's lymphoma is the more prevalent type, with an estimated 80,470 cases and estimated 20,250 deaths in the United States in 2022 (American Cancer Society, 2023; Siegel et al., 2022).

Diffuse large B cell lymphoma (DLBCL) is the most common type of adult and aggressive Non-Hodgkin's lymphoma (Hu et al., 2013; Li, et al., 2020). The treatment for DLBCL includes radiation, chemotherapy, and autologous stem cell transplantation. These treatments often do not resolve the genetic and epigenetic alterations that are characteristic of cancer. Therefore, targeting cellular factors to find a more targeted and less toxic method to treat DLBCL has been explored. Such cellular factors can be targeted to modulate cellular survival and division (Hu et al., 2013; Li, et al., 2020). One such factor is STAT3, which is targeted to reduce or eliminate DLBCL cells (Li et al., 2020; Schmitt et al., 2021).

### **Overview of STAT3**

In humans, there are seven STAT proteins: STAT1, 2, 3, 4, 5A, 5B, and 6 (Bharadwaj et al., 2014; Carpenter & Lo, 2014; Chai et al., 2016; Chalikonda et al., 2021; La Sala et al., 2020; Zhang et al., 2019a). All of them are involved in the JAK/STAT signaling pathway in response to myriad cytokines, growth factors and other signals (Li et al., 2020; Zhu et al., 2019). Among the STATs, STAT3 is pleiotropic and plays important roles in many cellular processes including proliferation and differentiation (Bai et al., 2019; Bharadwaj et al., 2014, Son et al., 2017). As a result, STAT3 has been shown to enhance oncogenesis, tumor growth, and progression (Arshad et al., 2020; Bai et al., 2019; Carpenter & Lo, 2014; Chai et al., 2016; Huang et al., 2014; Li et al., 2020; Lü et al., 2021). STAT3 mediates the expression of various genes that are involved in cancer cell survival, cell proliferation, migration, angiogenesis, invasion, metastasis, drug

resistance, apoptosis, immune evasion, and differentiation (Bai et al., 2019; Chalikonda et al., 2021; La Sala et al., 2020; Li et al., 2020; Lu et al., 2016; Zheng et al., 2021; Zhu et al., 2019). Abnormal activation of STAT3 is found in numerous types of cancer, including breast, pancreas, head and neck squamous cell carcinoma, leukemias, and lymphomas (Bharadwaj et al., 2014; Li et al., 2020; Zhu et al., 2019). In fact, STAT3 mutations have been associated with primary tumor growth and reduced overall survival in cancer patients (La Sala et al., 2020; Li et al., 2020; Shi et al., 2021). Aberrant STAT3 upregulation and activation is a common characteristic of lymphomas. Inactivation of STAT3 triggers apoptosis and achieves tumor regression in lymphomas (Bai et al., 2019; Li et al., 2020; Zhang et al., 2021). However, there are currently no FDA approved STAT3 inhibitors (Aigner et al., 2019; La Sala et al., 2020; Li et al., 2020; Lü et al., 2021; Yu et al., 2015; Zhu et al., 2019).

### **Structure of STAT3**

The human STAT3 gene is located on chromosome 17 (17q21.2), has 24 exons, and consists of 750-795 amino acids (Arshad et al., 2020, Liu et al., 2021, Shi et al., 2021). STAT3 and other STAT proteins have six domains: a conserved amino-terminus, a coiled-coil domain, a DNA-binding domain, a linker domain, the Src Homology 2 (SH2) domain, and a carboxy-terminal transactivation domain (TAD) (Figure 1) (Arshad et al., 2020; Chalikonda et al., 2021; Chai et al., 2016; Garcia-Reyero et al., 2021; La Sala et al., 2020; Liu et al., 2021; Mishra et al., 2021; Shi et al., 2021; Zhu et al., 2019). The SH2 domain is the key functional domain because it is involved in STAT3 dimerization and nuclear translocation (Chalikonda et al., 2021; La Sala et al., 2020; Liu et al., 2021; Mishra et al., 2021; Shi et al., 2021; Zhu et al., 2019). Phosphorylation at tyrosine 705 leads to STAT3 dimerization and nuclear translocation. Phosphorylation at serine 727 enhances the STAT3 transcriptional activity (Mishra et al., 2021; Zhu et al., 2019).

Other functional domains important for STAT3 functions include the amino-terminus (NTD) and coiled-coil domain (CC) (La Sala et al., 2020). The NTD mediates recognition of weaker DNA binding sites and formation of an antiparallel dimer using unphosphorylated STAT3 (Mishra et al., 2021; La Sala et al., 2020). The CC domain functions in nuclear translocation and has an important role in IL-22 receptor signaling (Mishra et al., 2021; La Sala et al., 2020). Lastly, the linker domain (LD) that occurs between the DNA binding domain (DBD) and the SH2 domain may play a structural role as an allosteric communicator between the two (Mishra et al., 2021; Mertens et al., 2020).

Four isoforms of STAT3 (Figure 1) have been identified:  $\alpha$ ,  $\beta$ ,  $\gamma$ , and  $\delta$  (Liu et al., 2021). The major isoforms are STAT3 $\alpha$  and STAT3 $\beta$  (Mishra et al., 2021; Zhu et al., 2019). STAT3 $\gamma$  and STAT3 $\delta$  are C-terminal truncated forms of STAT3 $\alpha$  and are thought to be produced through proteolytic processing (Liu et al., 2021). Each isoform has distinct biological functions which depend on cell type and context (Table 1) (Liu et al., 2021). All four isoforms are found to be expressed in diffuse large B-cell lymphoma with STAT3 $\alpha$  being the most abundant around 75%, then STAT3  $\beta$  around 10%, and the remaining isoforms contributing to around 15% expression combined (Turton et al., 2015).

**Figure 1. *STAT3 Functional Domains and Isoforms***



Isoform	Size	Function	Sources
STAT3 $\alpha$	770 aa, 92 kDa	Maximal transcriptional activation (due to dual phosphorylation); activation of target genes may result in recruitment of cofactors; major role in oncogenesis; less stable dimer formation	Bharadwaj et al. (2014), Liu et al. (2021), Turton et al. (2015), Shamir et al. (2020), Zheng et al. (2021), Zhu et al. (2019)
STAT3 $\beta$	722 aa, 83 kDa	Greater potential for constitutive activity; greater DNA binding affinity and more stable dimer formation; has some antitumor effects when overexpressed; modulates inflammation; reduce resistance to chemotherapy; forms complexes with other co-activators and STAT3 $\alpha$	Aigner et al. (2019), Bharadwaj et al. (2014), Liu et al. (2021), Shamir et al. (2020), Turton et al. (2015), Zhang et al. (2019a), Zheng et al. (2021), Zhu et al. (2019)
STAT3 $\gamma$	72 kDa	Regulation of granulocyte development; activated in terminal differentiated neutrophils, involved in regulation of cell proliferation	Liu et al. (2021), Shi et al. (2018)
STAT3 $\delta$	64 kDa	Regulation of granulocyte development-expressed in early stages	Liu et al. (2021), Shi et al. (2018)

### STAT3 in Cancer

STAT3 is a DNA binding transcription factor. In cancerous cells, STAT3 activation is common and has been frequently linked to more malignant cancer behaviors, including cell growth, epithelial-mesenchymal transition, migration, invasion, and metastasis (Bai et al., 2019; Carpenter & Lo, 2014; Chalikonda et al., 2021; Chai et al., 2016, Li et al., 2020; Zhang et al., 2021). STAT3 activation is also associated with tumor survival and therapeutic resistance (Carpenter & Lo, 2014; Chai et al., 2016). The mechanism of STAT3 in oncogenesis is still unclear and likely dependent on tumor type and cellular context (Mishra et al., 2021). However, STAT3 has been shown to induce lymphoma, melanoma, breast, prostate, lung, cervical, and skin cancers (Bharadwaj et al., 2014; Chalikonda et al., 2021; Carpenter & Lo, 2014; Huang et al., 2014).

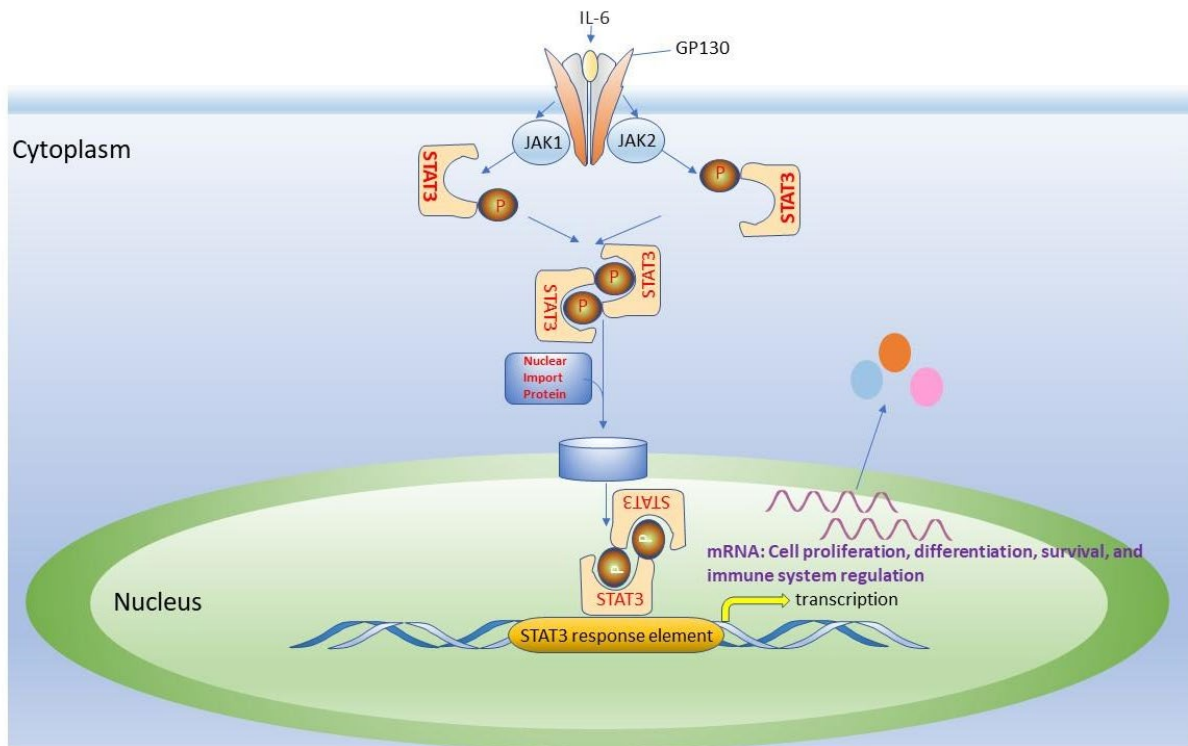
In lymphoma, STAT3 constitutive activation is particularly common (Zhu et al., 2019). STAT3 gain-of-function mutations have been shown to increase as a result of phosphorylation and transcriptional activity that promote malignancies (Chalikonda et al., 2021; Garcia-Reyero et al., 2021; Song et al., 2018b; Zhu et al., 2019). These mutations are associated with a variety of lymphomas and related auto-immune disorders (Zhu et al., 2019).

### ***Mechanism of STAT3 Signaling and Cancer Development***

STAT3 is involved in cellular signaling pathways including the JAK-STAT pathway that affects the growth, division, differentiation of cells, and immune responses (Lü et al., 2021, Li et al., 2020, Yu et al., 2015, Zhu et al., 2019). Specific cytokines (IL-6, IFN- $\alpha$ , etc.) and growth factors (EGFR, EGFRvIII, HER2 and PDGFR) can activate non-receptor tyrosine kinases (Src and all the JAK family proteins) to phosphorylate STAT3 at the Tyr705 residue (Arshad et al., 2020; Bai et al., 2019; Carpenter & Lo, 2014; Chalikonda et al., 2021; Li et al., 2020; Yu et al., 2015; Zhao et al., 2018). Phosphorylated STAT3 can then homodimerize or heterodimerize (with other STAT molecules) and translocate to the nucleus (Bai et al., 2019; Carpenter & Lo, 2014; Huang et al., 2014). In the nucleus, STAT3 binds to sequences within target gene promoters to activate gene transcription (Bharadwaj et al., 2014; Carpenter & Lo, 2014) (Figure 2). Under normal physiological conditions, STAT3 signaling is highly controlled by intracellular suppressors and various tyrosine phosphatases (Lü et al., 2021). However, STAT3 signaling can be affected by mutations that may lead to tumor progression (Lü et al., 2021). These mutations may be in the protein itself, upstream elements (G-protein receptor for cytokines/growth factors or JAK proteins) or downstream elements (immune system regulatory elements, cell growth and division genes, or other STAT3-induced genes).

Recurrent somatic mutations involving the SH2 domain of the protein may activate STAT3 by disrupting the autoinhibitory function of the SH2 domain, leading to constitutive STAT3 activation and increased presence of phospho-STAT3, (Garcia-Reyero et al., 2021). This may lead to overactive phosphorylation and dimerization of STAT3, thus upregulating other proteins involved in cell growth and division and immune system evasion, such as MYC and PD-L1, respectively (Chalikonda et al., 2021; Garcia-Reyero et al., 2021; Song et al., 2018b). Other mutations that affect the role of STAT3 in cancer in a tumor suppression manner include the linker domain and the DNA binding domain (Table 2).

**Figure 2. *STAT3 Signaling Pathway***



*Note:* Schematic representation of STAT3 signaling pathway through IL-6. IL-6 is a cytokine that binds to its membrane receptor, which activates non-receptor tyrosine kinases (JAK1, JAK2). These kinases phosphorylate STAT3 at Tyr705. The phosphorylated STAT3 molecules homodimerize and translocate to the nucleus, regulating genes involved in the immune response and cell growth/division.

**Table 2. STAT3 Mutational Effects**

STAT3 Mutation	Effect	References
----------------	--------	------------

<b>SH2 domain</b>	PhosphoSTAT3 (Tyr705) protein overexpression	Garcia-Reyero et al. (2021)
<b>Linker domain</b>	May suppress or induce STAT3 transcriptional activation and inhibits dephosphorylation	Mertens et al. (2020)
<b>DNA binding domain</b>	Suppresses STAT3 DNA binding and expression of target genes	Xiong et al. (2021)
<b>Coiled-Coil domain</b>	Increase STAT3 phosphorylation in STAT3 $\alpha$ mutant cell lines with no effect on the STAT3 $\beta$ mutant cell line	Hu et al. (2013)

Because of the various roles of the activated genes, STAT3 is known to be pleiotropic, meaning that one gene affects multiple phenotypes, and identifying the specific mechanism in each type of cancer has been a challenge for researchers (Aigner et al., 2019; Carpenter & Lo, 2014; Zhu et al., 2019). In common, when STAT3 is hyperactive, cell division rapidly occurs, which can potentiate the spread of cancerous cells and tumor growth (Liu et al., 2021; Zhu et al., 2019). One way STAT3 has a direct effect on cell proliferation is that it activates the expression of oncogenes including CDC2, MCL-1, survivin, BCL2, and PD-L1 (Song et al., 2018b; Zhu et al., 2019). These oncogenes affect checkpoints within the cell. In healthy, non-cancerous cells, there are multiple points throughout the cell growth and division process to ensure that all organelles and DNA are replicated properly (Zhu et al., 2019). However, when these oncogenes are active, they inhibit these checkpoints, which allows unhealthy, cancerous cells to proliferate at a quick rate instead of undergoing apoptosis, or programmed cell death (Yang et al., 2019). The promotion of oncogenes plays a direct role in the proliferation of cancer and is often supported by the hyperactivity of STAT3. In diffuse large B-cell lymphoma, the JAK/STAT3 pathway is constitutively active and leads to the expression of oncogenes (Zhu et al., 2019). A

similar process occurs in T-cell lymphoma in addition to mutations in STAT3, STAT5, and loss of function mutations in p53 and SOCS-1 (Zhu et al., 2019).

Additionally, constitutive STAT3 signaling may result in the immunosuppression of immune cells, leading to cancerous cell proliferation (Chalikonda et al., 2021; Garcia-Reyero et al., 2021; Lee et al., 2019, Lü et al., 2021; Proia et al., 2020; Zhu et al., 2019). Aberrant STAT3 activation can lead to inappropriate expression of genes involved in tumor immune evasion such as PD-L1, which renders T cells unable to mount an immune response (Chalikonda et al., 2021; Garcia-Reyero et al., 2021; Song et al., 2018b; Zhu et al., 2019). Furthermore, STAT3 encourages the polarization of macrophages associated with tumor growth such as M2 macrophages (Proia et al., 2020, Yang et al., 2019; Zhao et al., 2018). Polarization is the activation of the macrophage towards a specific phenotypic function. Macrophages can be classified into two major subtypes: classically activated pro-inflammatory, or M1 macrophages, and alternatively activated anti-inflammatory, or M2 macrophages (Yang et al., 2019). STAT3 activates the M2 phenotype and consequently results in angiogenesis and tumor progression through immunosuppression (Larionova et al., 2020). When STAT3 is inhibited, there is less macrophage polarization towards M2 (Lee et al., 2019). Because of STAT3's role in cell division, proliferation of cancerous cells, and immunosuppression, it is a promising therapeutic target for lymphoma and other cancers (de Araujo et al., 2020; Huang et al., 2014; Mishra et al., 2021; Li et al., 2020; Yang et al., 2019; Zhao et al., 2018; Zhu et al., 2019).

### ***Development of STAT3 Inhibitors for Cancer Treatment***

Pharmacological inhibitors targeting STAT3 can be either synthetic or natural and are generally categorized into different subclasses based on target sites (Chai et al., 2016). Current limitations of these inhibitors include lack of specificity and efficacy. One type of inhibition is

targeting the STAT3 DNA binding domain. STAT3–DNA interaction is necessary for STAT3-regulated gene expression (Chai et al., 2016). Thus, inhibition of the STAT3 DNA binding domain would potentially abrogate STAT3 activity, preventing STAT3-regulated gene expression (Chai et al., 2016, Son et al., 2017). Targeting the DNA-binding activity of STAT3, regardless of its phosphorylation and dimerization status, is a promising strategy. However, developing small molecules that can selectively disrupt protein-DNA interactions by targeting the DNA-binding domains (DBDs) of transcription factors is challenging (Huang et al., 2014). Another major category is inhibition of the SH2 domain (Garcia-Reyero et al., 2021, Huang et al., 2014). Since the SH2 domain is the major functional domain involved in STAT3 phosphorylation and dimerization, some small molecules have been developed to inhibit this domain and have reached the preclinical development stage (Bai et al., 2019, Mertens et al., 2020, Qi et al., 2020, Son et al., 2017, Yang et al., 2019, Yu et al., 2015).

However, there have been problems with using small molecules to target the SH2 and DNA binding domains, because some STAT3 dimerization and nuclear translocation may occur without phosphorylation of the tyrosine residue (Bai et al., 2019, Chai et al., 2016, Huang et al., 2014). Additionally, monomeric STAT3 has been shown to have some transcriptional activity (Bai et al., 2019, Huang et al., 2014, Mishra et al., 2021). Therefore, inhibiting STAT3 phosphorylation is unlikely to block the complete transcriptional activity of STAT3 (Bai et al., 2019, Huang et al., 2014). Another issue with blocking the SH2 domain specifically is its sequence homology in other STAT proteins (Bai et al., 2019, Son et al., 2017). As a result, it is hard to have a small molecule inhibitor specific to STAT3 (Bai et al., 2019, Son et al., 2017). Other levels of inhibition include suppression of the N-terminal domain/coiled-coil domain, marking STAT3 for degradation, or targeting other upstream/downstream signaling (Table 3).

One weakness with targeting upstream and downstream signaling such as JAK2 or oncogenes activated by STAT3 is off-target effects (La Sala et al., 2020, Son et al., 2017). That is why targeting the STAT3 protein directly is ideal. Degrading STAT3 may be a more promising therapeutic strategy. Tissue-specific deletion of STAT3 in adult mouse tissues has exhibited non-lethal phenotypes and even resulted in long-lasting tumor cell regression (Bai et al., 2019).

Lastly, there have been some studies that target STAT3 using antisense nucleotides (ASO) (Proia et al., 2020, Zhao et al., 2018). Recent advances in a combination of oligonucleotide chemistry and base modifications have led to safer, more selective, and potent oligonucleotides for target knockdown (Proia et al., 2020). Targeting STAT3 in this manner has influenced the tumor microenvironment and alleviated the immunosuppressive functions of STAT3 in patients and mice with B-cell lymphomas, especially in combination therapies with anti-PD-L1 approach (Proia et al., 2020, Zhao et al., 2018). Though this method is another promising approach to targeting STAT3 and inducing tumor cell death, ASO delivery to targeted cells is still a barrier to the clinical adoption of such an approach. This literature review focuses on protein-based inhibitors.

**Table 3. Preclinical and Clinical Stage STAT3 Protein Level Inhibitors for Cancer Treatment**

<b>Type of STAT3 Inhibition</b>	<b>Inhibitors</b>	<b>Significance</b>	<b>References</b>
N-terminal domain and coiled-coil domain	GRIM-19, MS3-6, and other STAT3 monobodies	Better understanding of mechanism and specificity behind STAT3 inhibition- there is diminished DNA binding and nuclear translocation, blocked transcriptional activation,	La Sala et al. (2020), Mishra et al. (2021)

		disruption of STAT3 interactions, and STAT3 degradation	
DNA binding domain	BOL, InS3-54, MMP, NTZ	Facilitate dephosphorylation of STAT3, blocks STAT3-DNA interaction and expression of STAT3 downstream target genes, induced apoptosis and tumor cell regression	Huang et al. (2014), Lü et al. (2021), Son et al. (2017), Wei et al. (2019)
SH2 domain	Eriocalyxin B, Rhein, Trichothecin	Inhibit STAT3 activation, phosphorylation, and dimerization, thereby blocking STAT3 nuclear translocation and transcriptional activity which results in cell growth inhibition and induces apoptosis	Qi et al. (2020), Yang et al. (2019), Yu et al. (2015)
Marking STAT3 for degradation	SD-36	Engagement with SH2 domain induces degradation and selectively degrades STAT3 in tested human cell lines	Bai et al. (2019)
Inhibit VEGF production	WP1066	Inhibition of p-STAT3 with WP 1066 results in the down modulation of multiple downstream transcriptional products.	Groot et al. (2022)*
Inhibition of upstream and downstream signaling	DMF, Eriocalyxin B, Napabucasin, TG101209	Downregulates expression of STAT3 target genes and prevents cell growth, migration, invasion, and angiogenesis	Li et al. (2020), Lu et al. (2016), Schmitt et al. (2021), Zhang et al. (2021)
STAT3 phosphorylation-exact mechanism unknown	Crocin, Napabucasin	Inhibits STAT3 phosphorylation and activation in cancer, increasing apoptosis, and decreasing secretion of chemokines/inflammatory factors	Li et al. (2020), Wang et al. (2020a)
Inhibit STAT3-driven gene	Napabucasin	Inhibit cancer stem cell activity with no adverse	Jonker et al (2018)**, Hubbard and Grothey

transcription and block spherogenesis		effects on hematopoietic stem cells and is the direct STAT3 inhibitor that has advanced into phase III trials.	(2017)
---------------------------------------	--	--	--------

\*phase I clinical trial NCT01904123

\*\*phase III clinical trial NCT01830621

As seen in Table 3, many STAT3 inhibitors have been studied over the past decade. Of these studies, there exists a limited number of direct and indirect inhibitors that have reached clinical trials (Zou et al., 2020). There are currently 67 clinical trials that are ongoing, terminated, or completed. Future development including more potent and selective STAT3 inhibitors for cancer therapy is needed (Bai et al., 2019, Lu et al., 2016, Proia et al., 2020, Qi et al., 2020, Yu et al., 2015, Zhu et al., 2019).

In this research, we intended to explore a viral protein as a STAT3 inhibitor. Past research has demonstrated numerous viral proteins with intrinsic tumor-specific toxicity (Wyatt et al., 2019). Some have even had the potential to degrade STAT3- one example is *Human Herpesvirus Type 6 (HHV-6) Rep6/U94* (Manocha & Caccuri, 2021). Though the mechanism of action of all these proteins is not fully understood, it is possible that they can manipulate several cell death modes in cancer, exemplifying the intricate interplay between these pathways (Manocha & Caccuri, 2021, Wyatt et al., 2019). Here, we explored the nsp5 protein of PRRSV for its role specifically relating to the degradation of STAT3 as a potential treatment for lymphoma. This viral protein has been shown to degrade STAT3 (Yang et al., 2017).

### Overview of nsp5

PRRSV is a single-stranded, positive-sense RNA virus that infects swine and causes reproductive failure in sows and respiratory diseases in pigs of all ages (Hu et al., 2021; Li et al.,

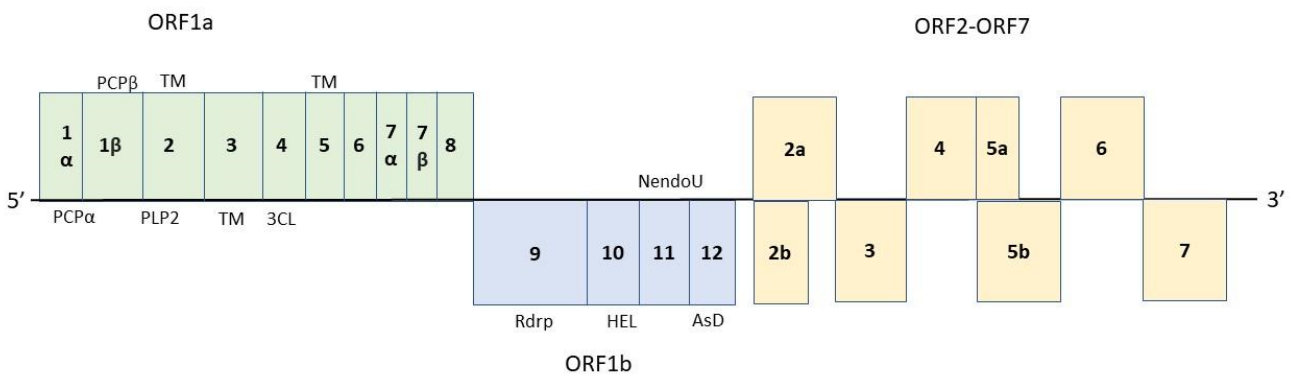
2015; Rascón-Castelo et al., 2015; Song et al., 2018a; Zhang et al., 2022). Nsp5 is one of the nonstructural proteins (Nsps) of this virus (Hu et al., 2021; Nan et al., 2018; Rascón-Castelo et al., 2015; Song et al., 2018a). In virus-infected cells, nsp5 congregates in membrane-associated replicase complexes, which drive viral RNA synthesis (Li et al., 2015; Nan et al., 2018, Rascón-Castelo et al., 2015; Song et al., 2018a). Nsp5 is a membrane protein that has been shown to induce autophagy, one potential pathway of cell death, in transfected cells (Song et al., 2018a; Zhang et al., 2019b). Nsp5 has also been shown to downregulate STAT3, which may contribute to viral pathogenesis (Yang et al., 2017). However, the exact mechanism by which nsp5 downregulates STAT3 is still unclear.

### **Expression of nsp5**

The genome of PRRSV is around 15-kb long containing over 10 open reading frames (Figure 3). At the 5' end of the genome are replicase genes, followed by genes that code for structural proteins (Hu et al., 2021, Nan et al., 2018, Song et al., 2018a). Nsp5 is encoded by open reading frame (ORF) 1, which includes ORF1a and ORF1b (Nan et al., 2018, Yang et al., 2015). Nsp5 localizes in the perinuclear region of the cytoplasm, specifically around the endoplasmic reticulum, which may relate to the function of the protein (Yang et al., 2015). The protein is predicted to have a molecular weight of about 18.9 kDa with 170 amino acids, most of which are hydrophobic and nonpolar (Nan et al., 2018, Song et al., 2018a, Yang et al., 2015). Nsp5 has been shown to interact with other non-structural proteins such as nsp7, nsp9, and nsp10 to induce some forms of inflammation (Rascón-Castelo et al., 2015, Song et al., 2018a, Song et al., 2020). It also functions in suppressing the JAK/STAT3 pathway and in inducing the autophagy process (Yang et al., 2017). The nsp5 inhibition of the STAT3 signaling is

independent of its autophagy induction, even though its overexpression leads to autophagic cell death (Yang et al., 2017).

**Figure 3. PRRSV Open Reading Frames**



*Note: Schematic illustration of PRRSV open reading frames (ORFs). Left to right: ORF1a, ORF1b, ORF2-ORF7.*

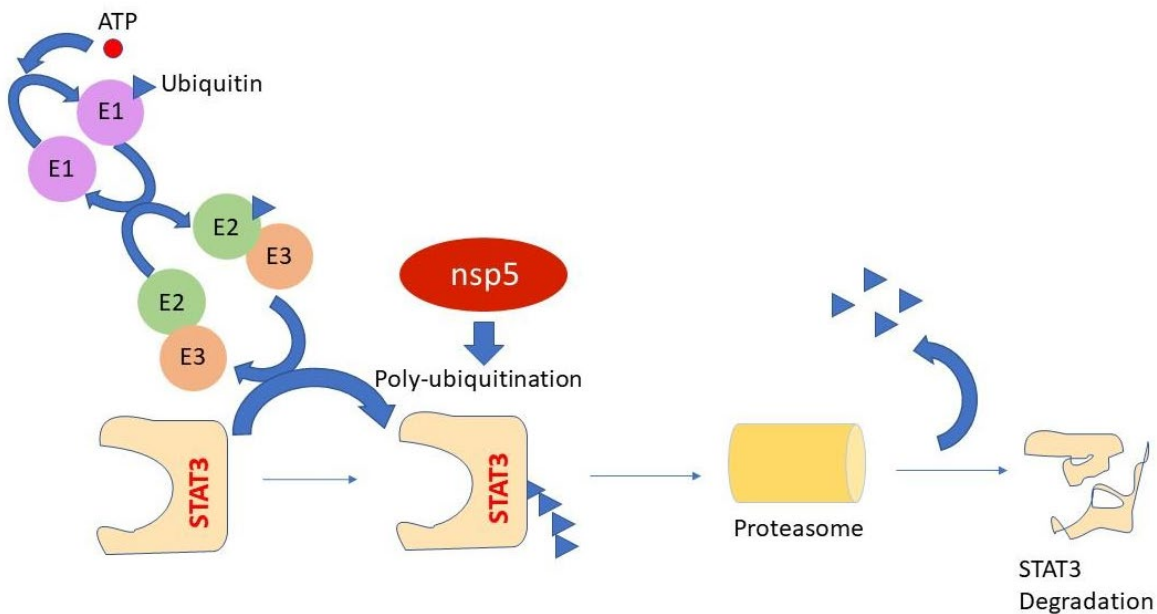
*ORF1a and ORF1b are labeled with nonstructural protein numbers (nsp). Nsp5 is encoded by ORF1a and contains a transmembrane (TM) domain. ORF2 to ORF7 are labeled by structural protein gene numbers. ORF1a and ORF1b are translated into pp1a and pp1ab which produce 14 nsp after proteolytic processing. ORF2 to ORF7 encode structural proteins involved in virion assembly. The following signature regions are indicated: RNA-dependent RNA-polymerase (RdRp), helicase (HEL), endoribonucleases (NendoU), and arterivirus-specific domain (AsD). Figure not drawn to scale. Inspired by Hu et al. (2021), Li et al. (2015), and Rascón-Castelo et al. (2015).*

### Effects of nsp5 protein on STAT3

Nsp5 has been shown to inhibit the gp130/JAK/STAT3 signaling pathway (Yang et al., 2017). There is speculation surrounding the C-terminal domain residues and their role in inducing STAT3 degradation (Yang et al., 2017). There are several theories as to how the nsp5 viral protein downregulates the STAT3 pathway, though the exact mechanism is still unknown (Yang et al., 2017). Nsp5 is thought to degrade STAT3 through the ubiquitin-proteasome pathway (Figure 4). Ubiquitin is a small protein that can be covalently attached to a target

protein to form a polyubiquitin chain (Alberts et al., 2015). The polyubiquitinated protein is then translocated to the interior of a proteasome, where it is digested into small peptides (Alberts et al., 2015).

**Figure 4. *Nsp5* Mediated *STAT3* Degradation**



*Note:* Schematic illustration of nsp5-mediated STAT3 degradation through the ubiquitin-proteasome pathway. E1, E2, and E3 are enzymes involved in this pathway. It is thought that nsp5 helps accelerate the poly-ubiquitination of STAT3 through interaction with an unknown E3 ligase.

It is presumed that nsp5 activates a ubiquitin E3 ligase of STAT3 and accelerates proteasome degradation of STAT3, though the E3 ligase has not been identified (Yang et al., 2017). It seems that the polyubiquitination of the STAT3 protein could lead to the degradation of this protein in the proteasome (Yang et al., 2017). According to an experiment done by Yang (2017), the addition of the proteasome inhibitor MG132 to the PRRSV-infected cells restored the STAT3 protein levels (Yang et al., 2017). These results suggest that PRRSV antagonizes the

STAT3 signaling by accelerating STAT3 degradation via the ubiquitin-proteasomal pathway (Yang et al., 2017).

The ubiquitin-proteasomal degradation of STAT3 shortens its half-life from 24 hours to 3.5 hours (Yang et al., 2017). Cells transfected with nsp5 plasmid have been found to have less STAT3, therefore implying STAT3's degradation as a result of nsp5 (Yang et al., 2017). And the C-terminal half of nsp5 (nsp5-D4) was found to be responsible for the STAT3 degradation. This mechanism can be explored for cancer treatment due to the fact that STAT3 is upregulated in many cancers, as discussed above.

By exploring nsp5-mediated STAT3 degradation, we intended to clone nsp5-D4 and deliver it to the target lymphoma cells. For gene delivery, we must use an optimal delivery method that is safe, efficient, and specific. The main gene delivery methods are detailed next.

### **Gene Delivery**

For gene delivery, both viral and non-viral delivery methods have been developed and used in *in vitro* models. While non-viral methods can be easily produced at a large scale, these methods suffer low delivery efficiency and may have some cell toxicity effects (Santiago-Ortiz & Schaffer, 2016). On the other hand, viral delivery methods have highly evolved mechanisms developed from the parent virus that allows them to efficiently recognize, infect, and produce stable gene expression in cells (Santiago-Ortiz & Schaffer, 2016, Wyatt et al., 2019). They have been promising for gene-based therapy, with a majority of them used in clinical trials (Santiago-Ortiz & Schaffer, 2016). Viruses enter cells and modify existing cell defense mechanisms, while maintaining a relatively long survival rate (Lukashev & Zamyatnin, 2016). These characteristics mean a tremendous possibility for gene delivery in cancer. Several types of viral vectors have been used and modified over the years to achieve safe, effective, and specific gene therapy:

Adenovirus (Ad), Adeno-associated virus (AAV), Newcastle Disease Virus (NDV), Retrovirus, and Lentivirus. The strengths and weaknesses of these vectors are detailed in Table 4.

Adenoviruses are non-enveloped, double-stranded linear DNA viruses that have icosahedral capsids composed of hexon, penton, and fiber proteins, which are responsible for the virus's properties and infection of host cells (Greber & Gomez-Gonzalez, 2021; Bulcha et al., 2021; Medina-Kauwe, 2013). Adenovirus enters cells via receptor-mediated endocytosis, facilitated by the binding of fiber proteins to cell surface receptors and the penton base to integrins, leading to the release of lytic proteins and subsequent entry into the cytoplasm and translocation to the nucleus (Greber & Gomez-Gonzalez, 2021; Bulcha et al., 2021; Medina-Kauwe, 2013; Zhao et al., 2021).

Adeno-associated virus (AAV) is a non-pathogenic single-stranded linear DNA virus with Rep and Cap genes that encode proteins for replication, packaging, and genomic integration, as well as capsid proteins that enable gene delivery (Xu et al., 2021; Santiago-Ortiz & Schaffer, 2016). AAV enters cells via interaction with surface glycan receptors and clathrin-mediated endocytosis, followed by nuclear translocation (Hacker et al., 2020; Berry & Asokan, 2016; Santiago-Ortiz & Schaffer, 2016).

NDV is a negative-sense, single-stranded RNA avian virus, which has been explored to express foreign genes, and has been tested in rodents and pigs safely. In addition, NDV has been shown to be oncolytic and explored for cancer treatment (Lara-Puente et al., 2021, Manocha & Caccuri, 2021, Sanchez et al., 2015, Vijayakumar et al., 2020, National Cancer Institute, 2013).

Retroviruses are RNA viruses that use reverse transcriptase to integrate into the host genome and contain three ORFs encoding structural proteins and replication enzymes (gag, pol, and env) (Lukashev & Zamayatnin, 2016; Vargas et al., 2016). Retroviral expression systems are

constructed using multiple plasmids or a packaging cell line to ensure safety and efficacy, with one plasmid carrying the gene of interest and others containing the genetic elements required for packaging (Bulcha et al., 2021; Vargas et al., 2016). While useful in integrating genetic information into rapidly dividing cells, research with retroviruses performed *in vivo* show a lack in specificity in regard to cell type which could lead to deleterious phenotypic effects (Vargas et al., 2016)

Lentiviruses, a type of complex retrovirus, use three plasmids for gene transfer, packaging, and enveloping (O’Keefe, 2021; Vargas et al., 2016). Lentiviral replication occurs via the transportation of the preintegration complex into the nucleus, allowing integration in both dividing and nondividing cells (O’Keefe, 2021).

**Table 4. Viral Gene Delivery Methods**

Method	Strengths	Weaknesses	References
Adenovirus (Ad)	<ul style="list-style-type: none"> <li>● High transduction efficiency</li> <li>● Not integrate into host cell chromosome</li> <li>● Broad host range</li> <li>● Transient transfection</li> <li>● Strong immunogenicity</li> <li>● 7.5 kb insertion capacity</li> </ul>	<ul style="list-style-type: none"> <li>● Preexisting immunity limits this vector’s utility</li> <li>● Complex for systemic administration</li> <li>● Gene expression is fast and transient</li> </ul>	Bulcha et al. (2021), Lukashev & Zamayatnin (2016), Sahoo et al. (2021), Song et al. (2021), Zhao, et al. (2021)
Adeno-associated virus (AAV)	<ul style="list-style-type: none"> <li>● Small genome- easy to manipulate</li> <li>● Lacks essential genes needed for replication</li> <li>● Various tissue targets</li> <li>● Commonly used for in vivo gene transfer</li> <li>● Not much vector-related toxicity, low immunogenicity</li> <li>● Prolonged and high level of transgene expression</li> <li>● Lack of pathogenicity, and strong safety profile</li> </ul>	<ul style="list-style-type: none"> <li>● Not ideal with <i>in vitro</i> models</li> <li>● Not very reproducible in clinical trials</li> <li>● Lack of scalable and economical vector production clear of impurities (costly)</li> <li>● Expression of transgene decreases over time</li> <li>● Pre-immunity</li> <li>● Unable to deliver large genes (&lt;4.7 kb)</li> </ul>	Bulcha et al. (2021), Challis et al. (2019), Lukashev & Zamayatnin (2016), Sahoo et al. (2021), Santiago-Ortiz & Schaffer (2016), Song et al. (2021)

Newcastle disease virus (NDV)	<ul style="list-style-type: none"> <li>● Can be produced at low cost</li> <li>● Avian virus- no pre-existing immunity</li> <li>● Impressive safety profile in phase I and II human clinical trials</li> </ul>	<ul style="list-style-type: none"> <li>● Safety concerns for avian industry- regulatory hurdles</li> <li>● Unable to deliver large genes (&lt;5 kb)</li> </ul>	Lara-Puente et al. (2021), Manocha & Caccuri (2021), PDQ (2013), Vijayakumar & Palese (2020)
Retrovirus	<ul style="list-style-type: none"> <li>● Good safety levels</li> <li>● Can be stably expressed</li> <li>● Can be applied <i>in vitro</i> and <i>ex vivo</i></li> <li>● Has specific sites of genomic integration</li> </ul>	<ul style="list-style-type: none"> <li>● May integrate near proto-oncogenic regions in the genome</li> <li>● Inability to transduce non-dividing cells</li> <li>● Fragile compared to AAV</li> </ul>	Lukashev & Zamayatnin (2016), Miller (2014), Song et al. (2021), Vargas et al. (2016)
Lentivirus	<ul style="list-style-type: none"> <li>● Permit long-term gene expression by integrating into host genome</li> <li>● Elicit relatively weak immune responses</li> <li>● Can transduce non-dividing cells</li> <li>● Low cytotoxicity</li> </ul>	<ul style="list-style-type: none"> <li>● Absence of preferential integration site</li> <li>● Safety concern about potential insertional mutagenesis/oncogenesis</li> <li>● Time consuming and more complex system than retroviral system</li> </ul>	Bulcha et al. (2021), Lukashev & Zamayatnin (2016), Sahoo et al. (2021), Song et al. (2021), Vargas et al. (2016)

In summary, each gene delivery method has its pros and cons. There is much more research detailing the optimization of these vectors for higher efficiency and safety. We are looking to use a vector that will transduce lymphoma cells effectively and result in good expression of nsp5. Thus, we focused on using the pLNCX2 retroviral vector, due to its applications *in vitro* and ability to allow for stable nsp5 expression. As seen in Table 4, retroviral vectors have both of these features. Additionally, this system is less complex than a lentiviral system, and has the potential to be scalable and safe for *in vivo* experiments. Lastly, there is no pre-existing immunity for retroviral vectors.

### Chapter 3. Methodology

This project has two aims to evaluate the effectiveness of nsp5 as a cancer treatment for lymphoma. Our first aim was to construct a retroviral vector for nsp5 delivery into lymphoma cells. Our second aim was to analyze the effects of nsp5 in lymphoma cells on STAT3 degradation.

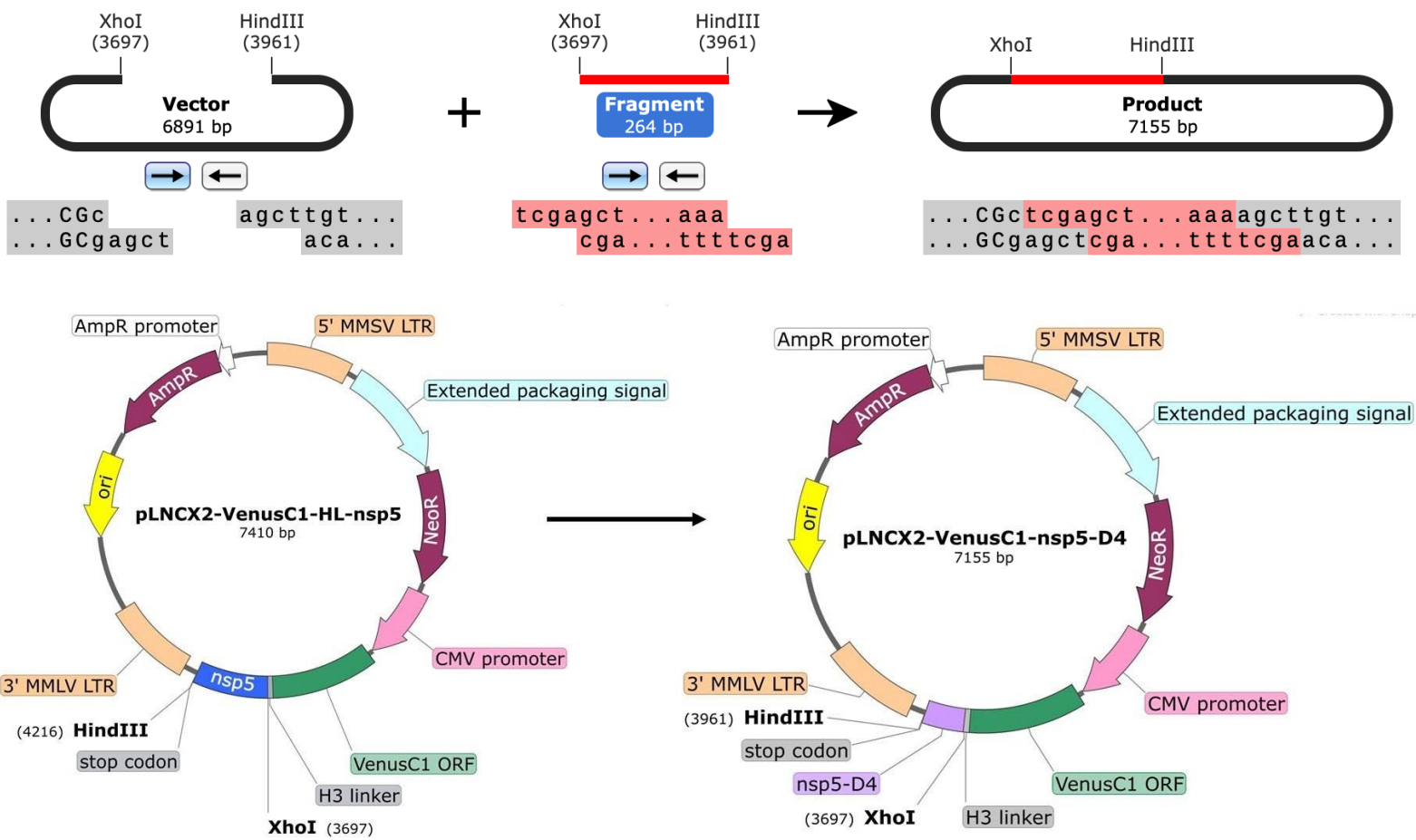
#### Plasmid Construction

The retroviral vector that was used in this project is the pLNCX2 (Takara bio) vector. Because pLNCX2 lacks a tag, the Venus gene was added to the vector so that transfection efficiency can be monitored using fluorescence microscopy. The recombinant pLNCX2-VenusC1-nsp5 vector was constructed before our joining the lab. We proceeded with cloning the nsp5-D4 sequence (encoding the C-terminal half of nsp5) to replace the full-length nsp5 in the pLNCX2-VenusC1-nsp5 vector. Our preference for this cloning method was based on the established preferred protocols and immediate availability of reagents in the lab. Specific details can be found in Appendix A.

PCR amplification of the nsp5-D4 segment (255 nt) was done using the forward primer 85nsp5F21 (5'CCTCGAGCTTGGTGCGGTGACCGGTTTTG 3') containing XhoI site and reverse primer 85nspR22 (5'CCGAAGCTTTTACTCGGCAAAGTACCGCAGG 3') containing HindIII site and stop codon. Restriction enzymes HindIII and XhoI were used to remove nsp5 from the pLNCX2-VenusC1-nsp5 vector and digest the amplified D4 fragment (Figure 5), followed by ligation and transformation. Bacterial colonies were screened for positive clones with PCR amplification using primers VenusC1-F1 (5'TGCTGCCCGACAACCACTACC3') and pLNCX2-R1 (5'TCACCGTCATCACCGAAACGCGCGAG3'). DNA was isolated from positive clones with GeneJET Plasmid Miniprep Kit (ThermoFisher Scientific) and subjected to

DNA sequencing with BigDye™ Terminator v3.1 Cycle Sequencing Kit (ThermoFisher) to confirm the presence of the D4 insert within the vector. The resulting recombinant plasmid DNA pLNCX2-VenusC1-nsp5-D4 was isolated with the PureYield™ Plasmid Midiprep System (Promega) for subsequent transfection experiments.

**Figure 5. Schematic illustration of pLNCX2-VenusC1-nsp5-D4 construction**



*Note:* Top: The pLNCX2-VenusC1-nsp5 (vector) and the nsp5-D4 insert (fragment) are cut with restriction enzymes HindIII and XhoI. Sticky ends in both fragments allow for the ligation and formation of pLNCX2-VenusC1-nsp5-

D4 of 7155 bp (product). Bottom: The initial and final product vectors. Since nsp5-D4 is smaller than nsp5, the product vector is smaller than the starting plasmid.

### **Transfection of GP2-293 cells**

The GP2-293 packaging cells were co-transfected with the transfer vector and envelope plasmid (pVSV-G). In this case, the transfer vectors are the control (pLNCX2-VenusC1) and the nsp5-D4 (pLNCX2-VenusC1-nsp5-D4). The GP2-293 cells were transfected right after splitting. The DNA transfection mixture was prepared and contained transfer vector DNA, VSV-G, and transfection reagent (polyethylenimine (PEI), JetOPTIMUS, or TransFectin). The mixture was incubated at room temperature for 20 minutes. During this process, the cells were trypsinized and resuspended in growth medium (Dulbecco's Modified Eagle Medium (DMEM) supplemented with 10% fetal bovine serum (FBS)). The dissociated cells were added to a cell culture plate. The DNA transfection mixture was then added to the cells and incubated for 48 hours. Fluorescence was observed at 24 h and 48 h after plating. The supernatant containing packaged retroviruses was then harvested. Further details on reagents, volumes, and times can be found in Appendix.

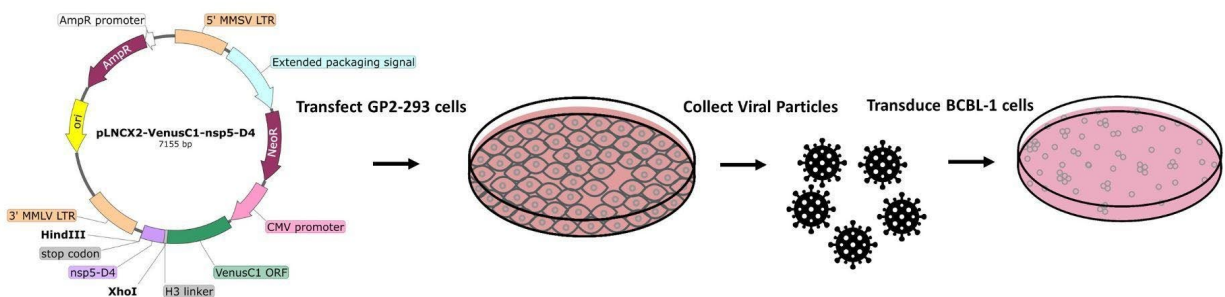
### **Reverse transcription and real-time PCR (RT-qPCR)**

To determine the retroviral titer in the harvested supernatant, we conducted RT-qPCR. RNA was isolated from the culture supernatant using Retrovirus Mini Purification Kit (BioVision) or PureLink™ RNA Mini Kit (Thermo Fisher Scientific) and treated with DNaseI to remove any residual DNA. Retro-X qRT-PCR Titration Kit (Takara) was used to determine the RNA copies in the purified RNA samples. More details can be found in Appendix B.4.

## Transduction of lymphoma cell line by retroviral particles

Once the recombinant retrovirus was harvested from the GP2-293 cells, the supernatant for the control (pLNCX2-VenusC1), and the nsp5-D4 (pLNCX2-VenusC1-nsp5-D4) was concentrated with the Retro-X™ Concentrator (Takara Bio) to increase the retrovirus concentration and thus increasing efficiency of the transduction. BCBL-1 cells were then transduced (Figure 6). BCBL-1 cells were plated in a culture plate with growth medium (Roswell Park Memorial Institute (RPMI1640) supplemented with 10% fetal bovine serum (FBS)). Polybrene (Sigma), a polycation, was used to increase the efficiency of the transduction. Concentrated retrovirus was then added to the target BCBL-1 cells and incubated for 72 hours. Fluorescence was observed at 24 h, 48 h, and 72 h after plating. The cells and supernatant were harvested at 72 hours post-transduction for further analysis. Further details on transduction can be found in Appendix.

**Figure 6. Schematic illustration of Transfection and Transduction**



*Note:* GP2-293 packaging cells were transfected with the nsp5-D4 plasmid for production of the recombinant retroviruses. BCBL-1 lymphoma cells were then transduced by the recombinant retroviruses to test the effect of the viral protein.

## Western Blot Analysis

Ultimately, we analyzed the expression of nsp5 and its effects on STAT3 protein levels in lymphoma cells. To determine the STAT3 protein level, lymphoma cells were lysed in Laemmli sample buffer and subjected to SDS-PAGE and western blotting, using primary antibodies against STAT3, GFP, and GAPDH. Blots were probed with secondary antibodies conjugated with horseradish peroxidase and imaged using chemiluminescence signal capture. This technique, adapted from Yang et al. (2017), allowed for the detection of nsp5 and the STAT3 protein level in the lymphoma cells.

## Cell Viability Assessment

A cell viability assay was run on transduced samples to assess the impact of the nsp5-D4 plasmid on cell health. Cells were transduced in a 24-well plate with a predetermined number of cells. To do so, BCBL-1 cells were counted to obtain the number of living cells per mL. Then, the desired number of cells were added to the 24-well plate. For this experiment 12 wells were used. Triplicates were run for each test as determined by two variables. Two were delivered  $5 \times 10^5$  BCBL-1 cells, while the other two were delivered  $1 \times 10^6$  cells. For each cell quantity group, one well was transduced with the empty vector and one well was transduced with recombinant viruses containing nsp5- D4. The transduction protocol for the cells is identical to the one described above. The supernatant for this experiment was not concentrated. The cells were harvested at 48h, with 25 uL of each well after ensuring homogenous cell distribution in the media were utilized for cell viability assay. The cell viability assay functions by detecting the number of living cells in a cell sample. The number of cells in a sample directly correlates to the signal detected by the CellTiter-Glo® Luminescent Cell Viability Assay (Promega). Three

readings of the luminescence were performed for each well, and the average of those readings was used.

## **Chapter 4. Results**

### **Cloning of nsp5-D4 into pLNCX2-VenusC1**

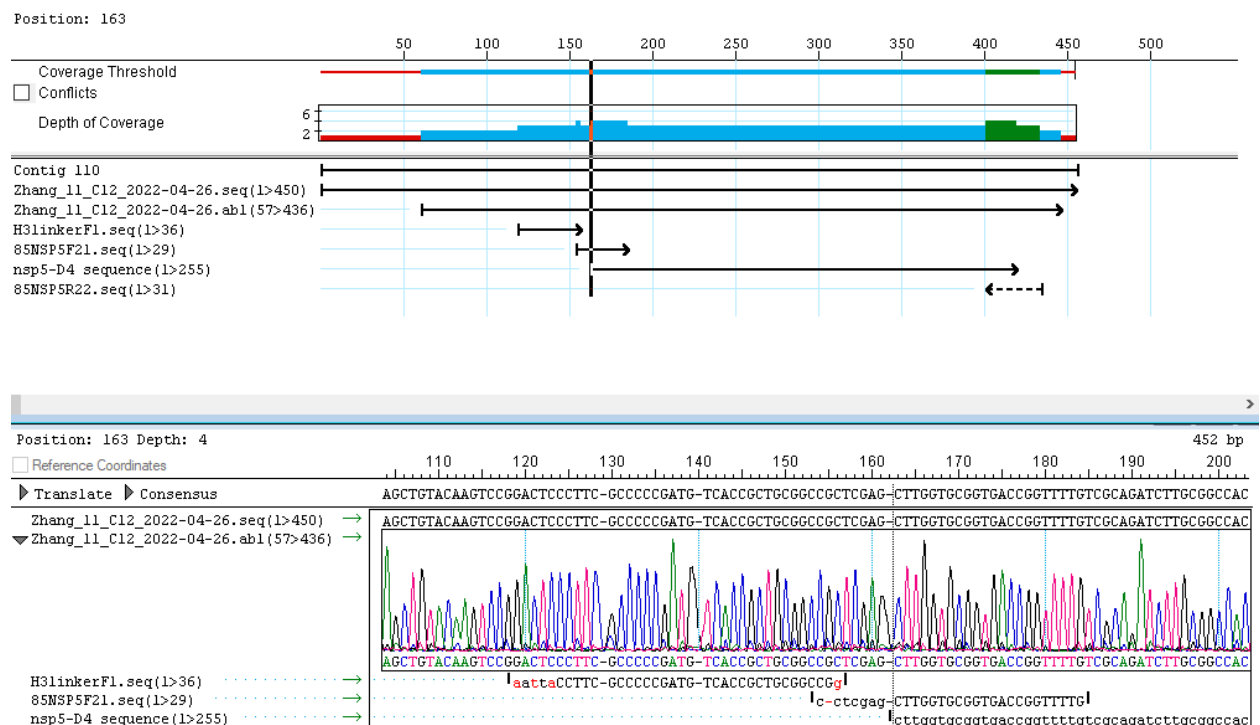
The nsp5-D4 was ligated into the pLNCX2-VenusC1 vector and colonies were screened for positive clones that contain nsp5-D4 according to the methodology in chapter 3. PCR and gel electrophoresis indicated nsp5-D4 was present (Figure 7). Twelve samples were run on a gel along with positive nsp5-D4 controls. Eight colonies were tested on March 7, 2022, and four more colonies were tested on March 9, 2022. All were from the same ligation. The length of the nsp5-D4 sequence is 255 bp. The colony PCR results show that 10 of the 12 samples had the band around 255 bp in the gel, in line with the positive controls. Out of the 10 positive samples seen in the gel, four were chosen for DNA isolation and sequencing. The DNA sequencing result showed the presence of nsp5-D4 insert in the positive clones (Figure 8). This portion of the Sanger sequencing shows the site of insertion of the nsp5-D4 sequence into the pLNCX2-VenusC1 plasmid. The alignment of the nsp5-D4 sequence in the plasmids with the original nsp5-D4 sequence showed they were identical.

**Figure 7. Gel Electrophoresis of Colony PCR**



*Note:* Image of agarose gel electrophoresis of the PCR screening for colonies from the pLNCX2-VenusC1-nsp5-D4 vector ligation. PCR samples from March 7 and March 9, 2022 were run. Positive control was included. Expected PCR products are seen around 255 bp.

**Figure 8. Alignment of D4 insert in pLNCX2-VenusC1-nsp5-D4 with original nsp5-D4**



*Note:* Sanger DNA sequencing of pLNCX2-VenusC1-nsp5-D4 confirms the presence of D4 in the plasmid. The top alignment figure depicts the plasmid sequenced (Zhang\_11\_C12...) and shows alignment to the nsp5-D4

sequence, and the forward and reverse primers. The bottom chromatogram depicts the sequence reads of the plasmid DNA.

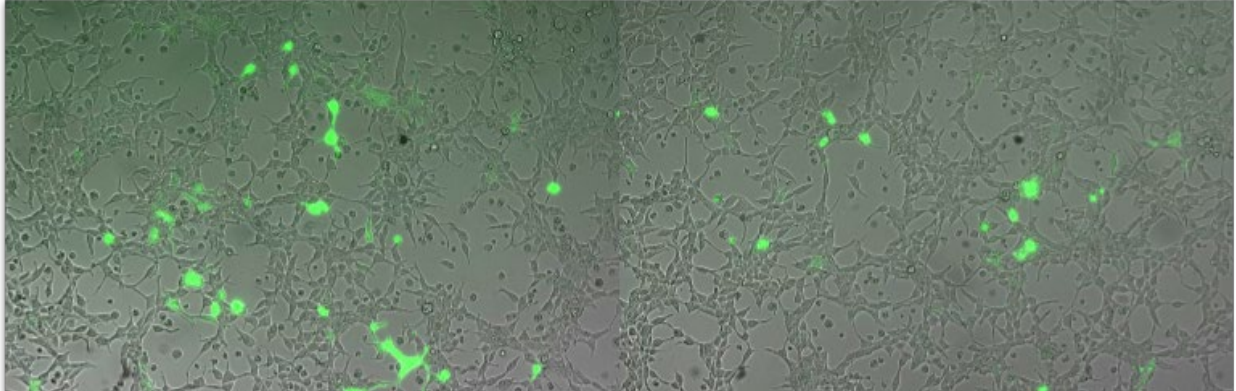
## **Optimization of Retroviral Packaging**

There are many different reagents that facilitate plasmid entry into the cells. The three reagents we attempted to optimize were Polyethylenimine (PEI), Polyplus jetOPTIMUS, and BioRad Transfectin. Next we describe the optimization of transfection with these different reagents.

### ***Polyethylenimine (PEI) Transfection***

Transfections were initially performed using polyethylenimine (PEI) as the transfection reagent for it has been used successfully in the lab. PEI is a chemical transfection reagent that works by complexing with DNA before being introduced to cells. These complexes facilitate the DNA's entry into the cells. The ratio of PEI:DNA is vital to the efficiency of transfection. The PEI to DNA ratio used was 6:1. Figure 9 displays the results of this transfection. The control vector containing only the gene encoding for VenusC1 is on the left and the vector containing nsp5-D4 is on the right. Cells transfected with either vector exhibited a low fluorescence rate, below 5%, indicating that not enough PEI complexes made it into the cells and that our transfection was unsuccessful. A better transfection reagent was necessary to improve the transfection efficiency.

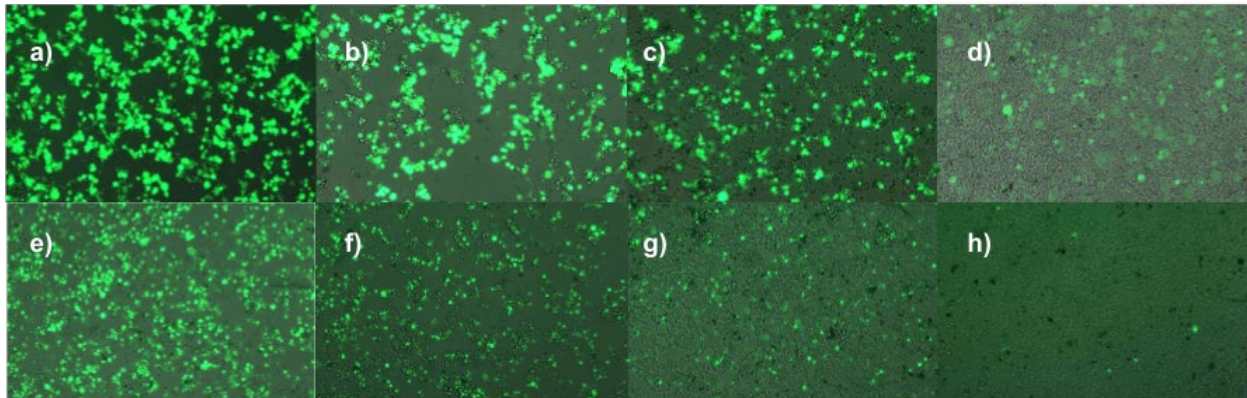
**Figure 9. *GP2-293 Transfection with PEI***



*Note:* Results of transfection with PEI. On the left is pLNCX2-VenusC1 and on the right is pLNCX2-VenusC1-nsp5-D4. The fluorescence rates in both of these images are very low.

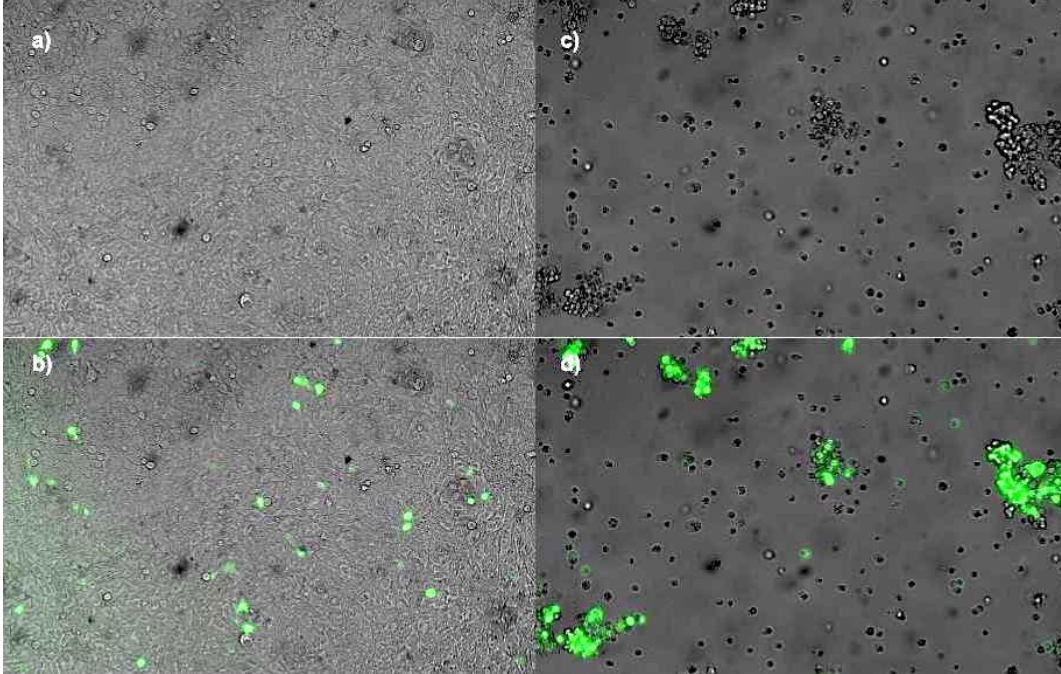
### ***Polyplus jetOPTIMUS Transfection***

The jetOPTIMUS from Polyplus is a polymer-based transfection reagent that the manufacturer claims is effective at transfecting a variety of cell lines. It works in a similar way to PEI: by forming complexes that then facilitate the DNAs entry into the cells. Initial transfections were focused on discovering the best VSV-G:DNA ratio to use in subsequent experiments. The results of the experiment are seen in Figure 10. We observed that as VSV-G increased in proportion to the plasmid DNA amount, the fluorescence rate decreased and the cell health, indicated by the confluency of the cells, increased. We found the optimal VSV-G:DNA ratio to be 0.8 $\mu$ g:1.0 $\mu$ g as that yielded the best balance between cell health and transfection efficiency. Figure 11 shows a comparison of transfections with PEI and Polyplus jetOPTIMUS. In the PEI pictures, the cells are confluent in the wells but exhibit low fluorescence. In the jetOPTIMUS pictures, cells are not confluent as indicated by the abundance of space between cells, but the cells exhibit significantly more fluorescence. These results show that jetOPTIMUS is too toxic to the cells. Our optimization including removing transfection mixtures from the cells four hours after adding them to the cells was unable to generate expected results. So we moved on to try another transfection reagent.

**Figure 10. GP2-293 Transfection using jetOPTIMUS with varying ratios of VSV-G:DNA**

*Note:* Fluorescence of the VSV-G:DNA ratio experiments. The top row, a-d, are of the control plasmid pLNCX2-VenusC1 and the bottom row; e-h, are of the experimental plasmid pLNCX2-VenusC1-nsp5D4. The columns represent different VSV-G:DNA ratios. From left to right, the ratios are 0.6:1.0, 0.8:1.0, 1.0:1.0 and 1.2:1.0, respectively.

**Figure 11. PEI vs jetOPTIMUS Comparison**

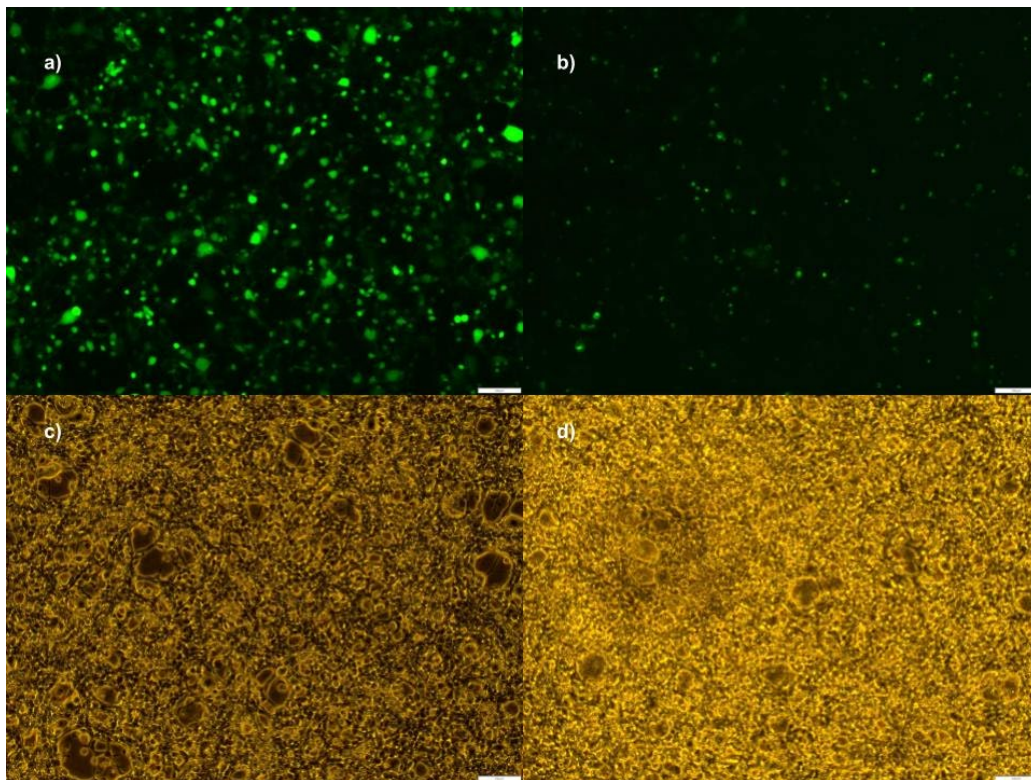


*Note:* Comparison of Polyplus jetOPTIMUS and PEI transfection reagents on GP2-293 cells. Images a and b are of PEI transfection, c and d are of jetOPTIMUS transfection. Images b and d are the overlaid fluorescence and brightfield microscopy images where a and c are just the isolated brightfield images.

### ***Bio-Rad TransFectin Transfection***

TransFectin is a lipid-based transfection reagent from Bio-Rad that works by enveloping the DNA and facilitating the entry of DNA into the cell through endocytosis. Results shown in figure 12 show the fluorescence following transfection using TransFectin. The brightfield images show confluent cells for both the empty vector and the nsp5-D4 vector and the fluorescent images show comparable fluorescence to our Polyplus jetOPTIMUS transfections for both vectors. These results show that Bio-Rad TransFectin is the best transfection reagent we tested. TransFectin was the reagent we continued with for the remainder of the experiments.

**Figure 12. GP2-293 Transfection with TransFectin**



*Note:* Fluorescence of transfection with BioRad TransFectin. Images a and b are the fluorescence images for the pLNCX2-VenusC1 and pLNCX2-VenusC1-nsp5-D4 vectors, respectively, and images c and d are the brightfield images for the same vectors.

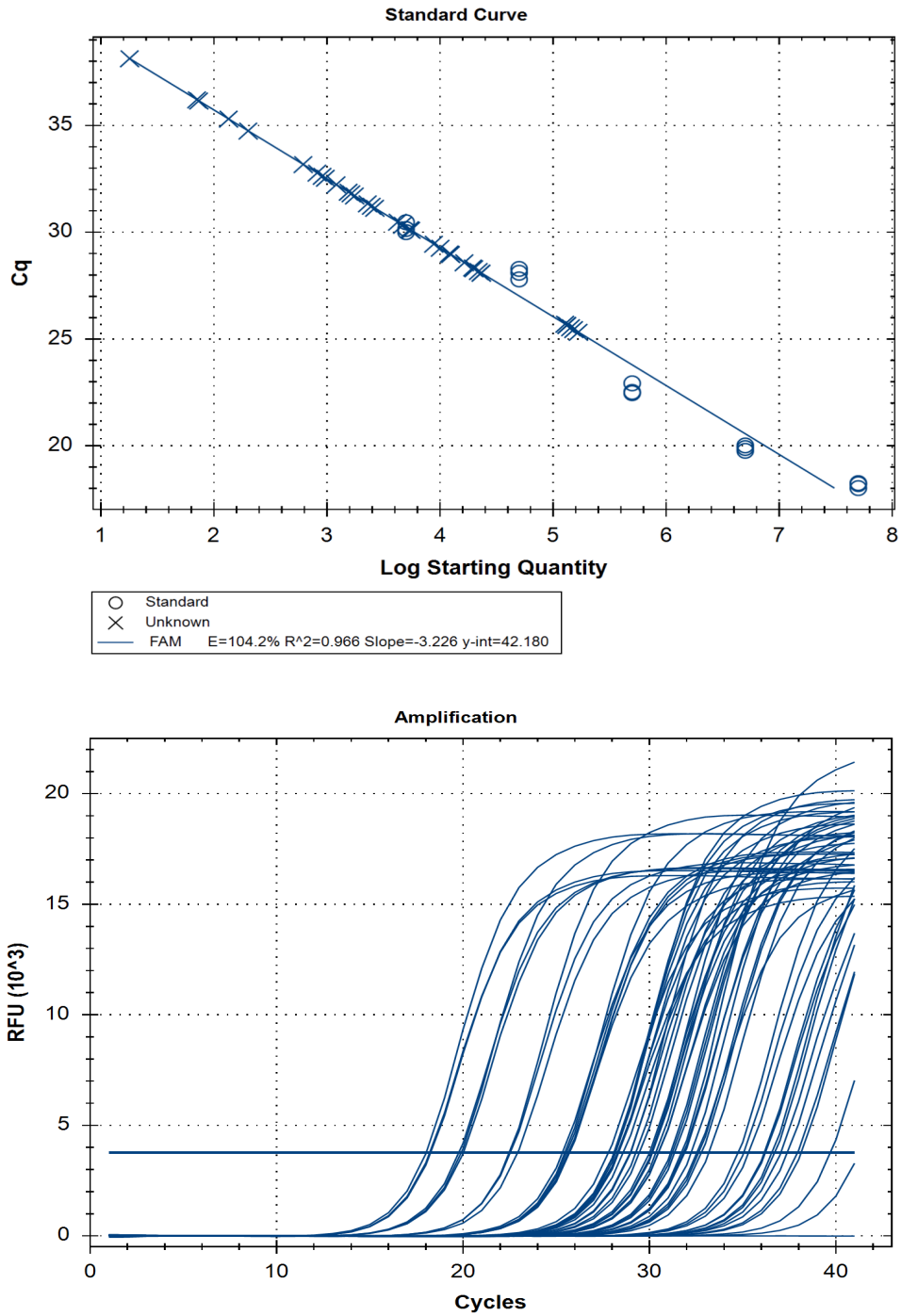
### **Retrovirus Titration**

After transfection of the GP2-293 cells, a retroviral titration kit was utilized to quantify the amount of viruses produced that contain packaged nsp5. This step helped ensure that retroviruses were produced by the transfection and estimate the amount of supernatant needed for transduction. The retroviral titration performed on January 19, 2023, showcases a standard curve, cycle threshold (Ct) values of the testing samples, and amplification curve in Figure 13,

indicating the detection of pLNCX2 (empty vector), pLNCX2-nsp5 (full length), and pLNCX2-nsp5-D4 in the supernatant of the GP2-293 cells after transfection with our vectors performed on January 3, 2023.

Running the real-time PCR allowed us to plot the Ct values compared to the known RNA starting quantities. As such, we were then able to determine the copy numbers of RNA in testing samples by comparing them to the standard curve. However, in order to draw these comparisons, it is necessary to evaluate both the linearity and the efficiency of the PCR. The slope of the standard curve was -3.226, a little less than the ideal -3.333. The  $R^2$  value was 0.966, which indicates the coefficient of correlation between the Ct and the RNA dilutions in the standard curve. The results showed the concentrations of RNA in the testing samples by comparing their calculated Cq values with that of the standard curve, providing the average copy number per microliter for the empty vector, full-length, and nsp5-D4 as follows: 7307.76, 991.67, 6972.59. The titer was from supernatant from the transfection performed on January 19, 2023, as seen in Figure 14.

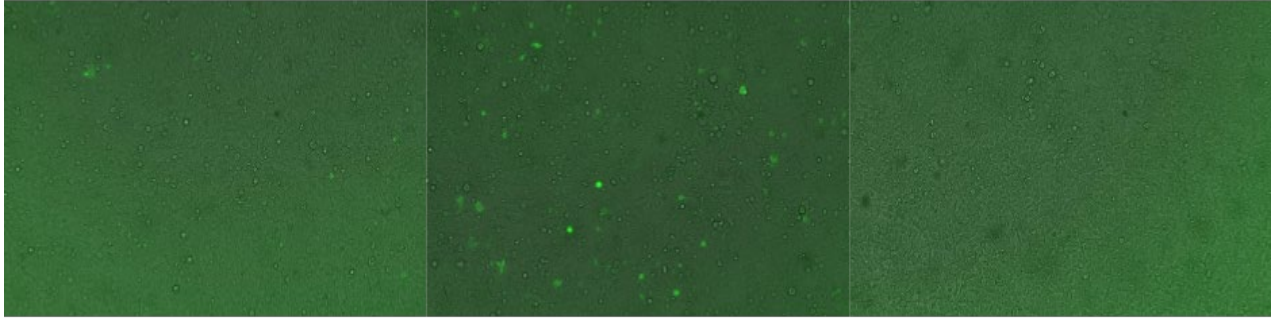
**Figure 13. *RT-qPCR Standard Curve and samples from GP2-293 transfection***



Note: Top: Standard curve of the RT-qPCR results found with our transfection supernatant from January 3, 2023.

Bottom: Amplification curve from the RT-qPCR run with the standard curve shown on top.

**Figure 14. GP2-293 Transfection with TransFectin**



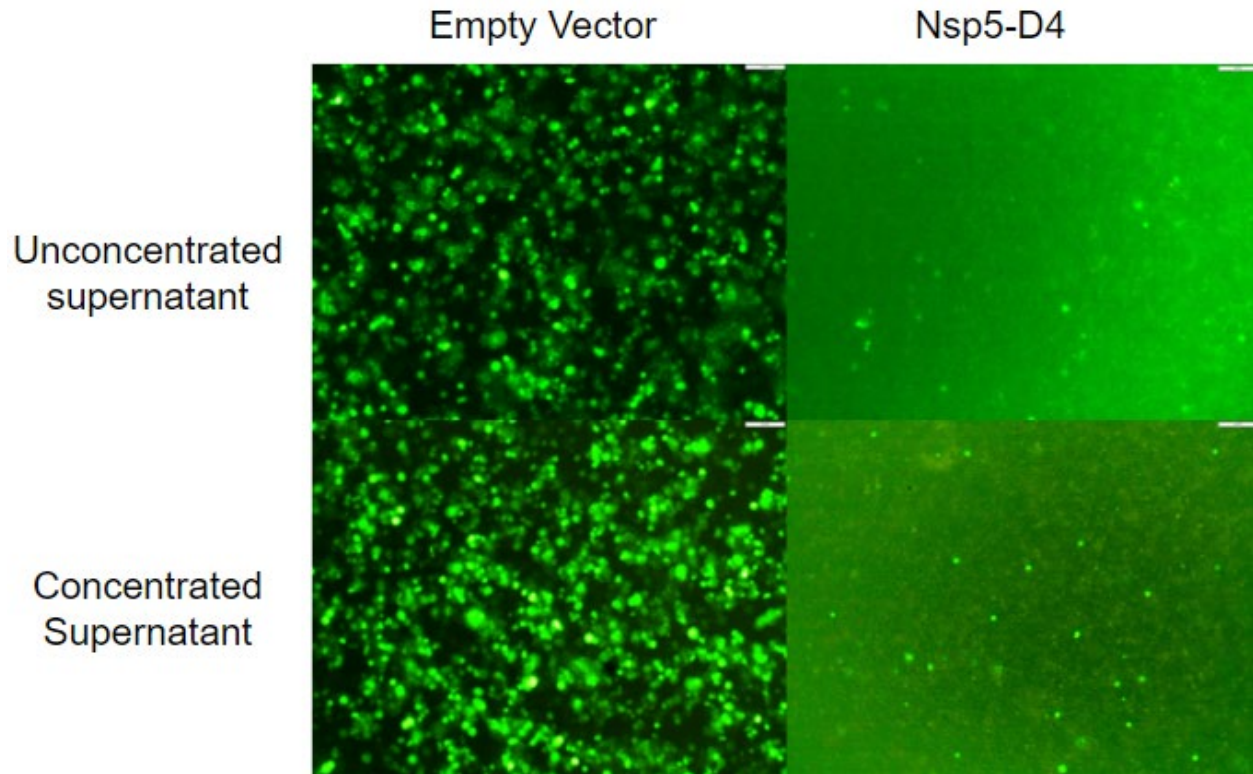
*Note:* These pictures were taken by using the fluorescent microscope specifically with the samples from the January 3, 2023 transfection that were used for the January 19, 2023 run of the RT-qPCR. These pictures allowed us to compare the average copy number per microliter of the empty vector, full-length, and nsp5-D4 as follows: 7307.76, 991.67, 6972.59 (quantification determined through RT-qPCR) in a visual manner. Left: Fluorescence of transfection with pLNCX2-VenusC1-nsp5-D4, Center: 24h fluorescence of transfection with pLNCX2-VenusC1 (empty vector) Right: fluorescence of pLNCX2-VenusC1-nsp5.

## **Transduction**

Recombinant retroviruses were delivered to BCBL-1 lymphoma cells. BCBL-1 cells were counted and a specific volume of GP2-293 supernatant was combined with a known number of BCBL-1 cells in RPMI medium. Polybrene reagent was added to increase transduction rates. Polybrene functions by providing cations that neutralize and lessen the repulsive interactions between the virus particles and the cancer cell surfaces. That enables better affinity between the envelope protein of the virus and the surface of the target cell.

To further increase transduction efficiency, retroviral supernatant was concentrated using a retroviral concentration kit by about 10-fold. By concentrating the supernatant, the number of viruses per mL of supernatant is expected to increase, enabling a larger number of viruses to be delivered to the BCBL-1 cells. The effectiveness of concentrating retroviral supernatant is assessed (Figure 15), which shows marginal improvement in transduction efficiency. A further experiment is needed to optimize the concentration and transduction of BCBL-1 cells.

**Figure 15. *Transduction efficiency of concentrated supernatant vs unconcentrated***



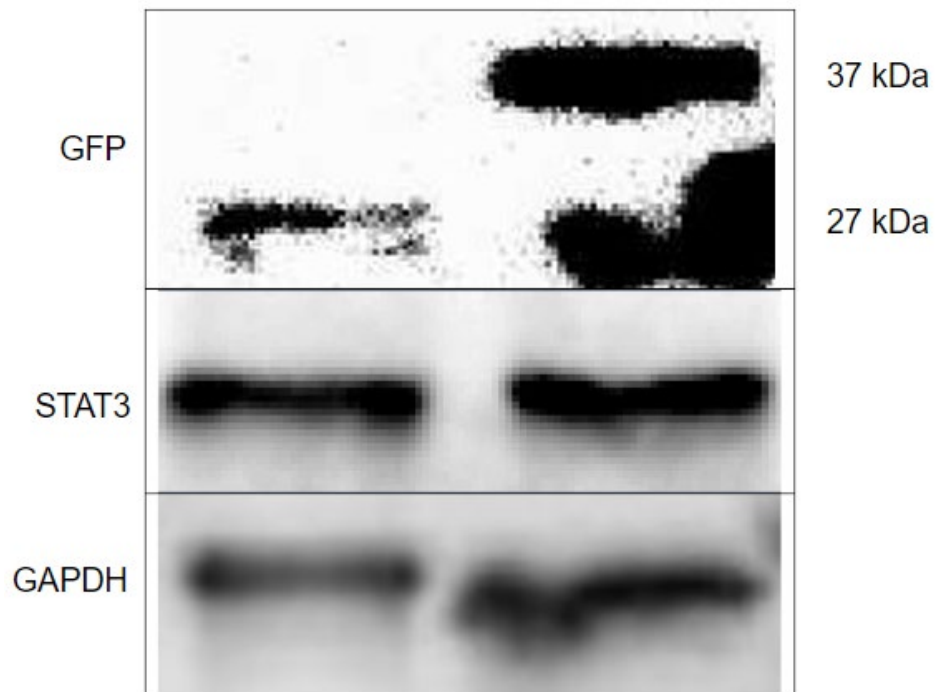
*Note:* BCBL-1 cells transduced with retrovirus from pLNCX2-VenusC1 (empty vector) and pLNCX2-VenusC1-nsp5-D4 vectors.

### **Western Blotting Detection of STAT3**

Western blot analysis was performed on the cell samples of both the transfected GP2-293 cells and the transduced BCBL-1 cells to determine the STAT3 protein in each sample. The levels of STAT3 protein were compared between the two different plasmids for each cell type. Nsp5-D4 is expected to reduce STAT3 levels in both cell types. Figure 16 shows one set of blotting images for BCBL-1 cell lysates. GAPDH levels were different between the two samples tested and used as the basis of the amount of protein in each lane. The relative intensity of GAPDH signals was used to normalize the amount of STAT3 in each lane. Figure 17 depicts the densitometry analysis for the images of western blot in Figure 16. Nsp5-D4 retrovirus reduced

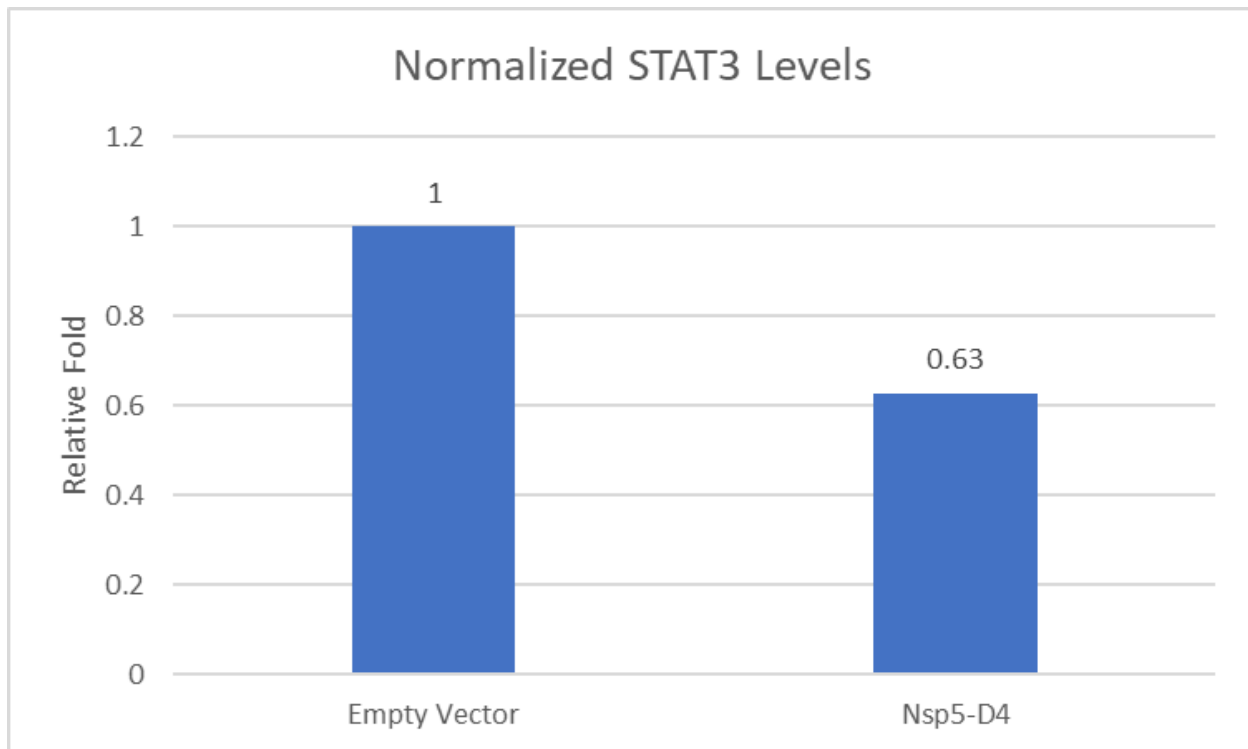
STAT3 level by 37% in this experiment. Further optimization is needed to improve the transduction and STAT3 reduction effect.

**Figure 16. Western blotting detection of STAT3 in BCBL-1 cells**



Note: Samples were taken from BCBL-1 cells that were transduced with concentrated retroviral supernatant. Left: empty vector. Right: nsp5-D4 vector. GFP-tagged Nsp5- D4 is 37 kDa and VenusC1 is 27 kDa in size. Noise signal is exhibited at 27 kDa in the nsp5-D4 lane due to gel running issue in the next adjacent lane to the right for the gel.

**Figure 17. Densitometry analysis of STAT3 protein level in BCBL-1 cells**

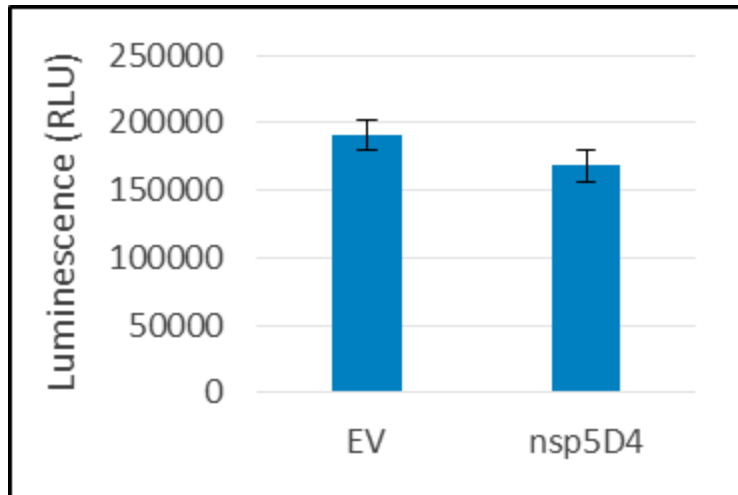


*Note:* Samples were taken from BCBL-1 cells that were transduced with concentrated retroviral supernatant. Nsp5-D4 induces a 37 percent decrease in STAT3 when normalized with GAPDH.

### Cell Viability Assay

The BCBL-1 cells transduced with the retroviruses were used to determine cell viability with a commercial kit. The cells were resuspended 48 hours after transduction and 25  $\mu$ l cell suspension were transferred to a 96-well testing plate for cell viability assay. Their relative luminescence values directly correlate with the number of cells in each well.

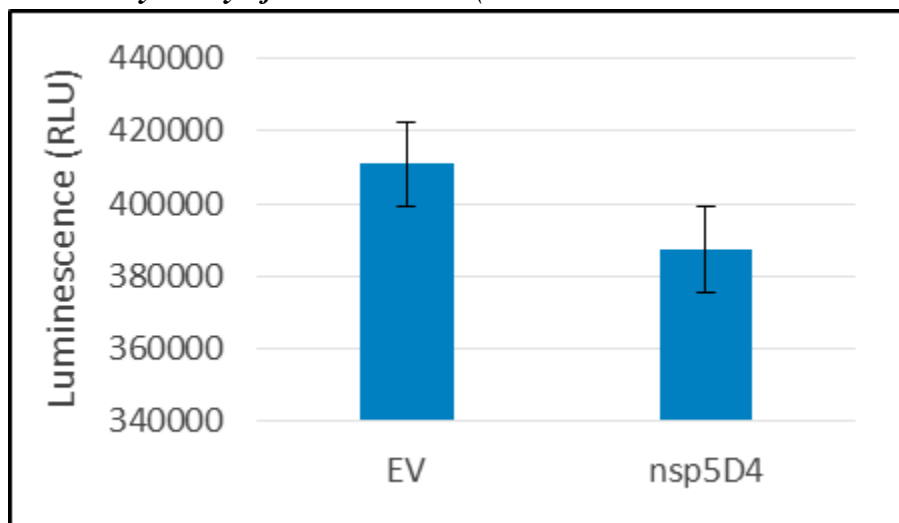
**Figure 18.** *Cell Viability Assay of BCBL-1 Cells ( $5 \times 10^5$  cells were transduced with retrovirus)*



Note: The RLU value correlates with the number of viable cells in the well 48h after transduction. These wells were seeded with  $1 \times 10^5$  cells.

For the wells containing  $5 \times 10^5$  cells upon transduction, the well that was infected with the retrovirus containing nsp5-D4 was 12 percent lower in luminescence than the control, indicating slightly reduced live cells.

**Figure 19. Cell Viability Assay of BCBL-1 Cells ( $1 \times 10^6$  cells were transduced with retrovirus)**



Note: The RLU value correlates with the number of viable cells in the well 48h after transduction. These wells were seeded with  $1 \times 10^6$  cells.

The wells containing  $1 \times 10^6$  cells when transduced exhibited a similar trend. Here, the number of cells in the nsp5-D4 well is 6 percent less than those in the control well. Both of these results suggest that the presence of nsp5-D4 reduces the viability of the BCBL-1 cells.

## **Chapter 5. Discussion**

### **Cloning of nsp5-D4 into pLNCX2-VenusC1**

The nsp5-D4 gene was successfully cloned into the pLNCX2-VenusC1 retroviral vector. The colony PCR gel result depicts a band of around 255 bp, which is the size of the nsp5-D4 segment. This indicates that the nsp5-D4 segment is within our plasmid of interest because the band would be larger if it was full-length nsp5. However, the gel run on the colony PCR samples is not ideal. It was over-run, which produced a low-quality image with much wider bands than expected. There were issues with gel electrophoresis to produce a high-quality image. DNA sequencing with the positive colonies gives us confirmation that the nsp5-D4 was inserted into the pLNCX2-VenusC1 plasmid correctly. The portion of the plasmid sequence where the nsp5-D4 insert is located shows a successful alignment. The Sanger sequencing results match the beginning of the nsp5-D4 sequence, which is how we know nsp5-D4 was correctly inserted. It was vital to ensure that nsp5-D4 was cloned successfully because it was found that nsp5-D4 is the portion that contains the critical amino acids which affect STAT3 degradation (Yang et al., 2017). Therefore, this vector can be used alongside the pLNCX2-VenusC1-nsp5 vector previously constructed to understand if the rate of STAT3 degradation is different within lymphoma cells.

## Optimization of Retroviral Packaging

Successful transfections involve balancing cell health with the cytotoxicity that accompanies the transfection reagent. With PEI, we observed low rate fluorescence and thus low transfection efficiency, indicating that not enough PEI complexes made it inside the cells. When we switched to Polyplus jetOPTIMUS, we observed a very high rate of fluorescence, but significant cell death that could not be mitigated by using different amounts of reagent or replacing media post-transfection. When comparing the fluorescence observed in PEI transfections in Figure 9, it is clear that the jetOPTIMUS transfections were more effective. As the transfection vessel was scaled up, however, the cells began to die in the plate. After numerous attempts to improve packaging cell health during jetOPTIMUS transfection including replacing media several hours post-transfection, we ultimately concluded that jetOPTIMUS was too toxic and therefore unsuitable for our needs in this process. It was only when we switched to lipid-based Bio-Rad TransFectin that we observed substantial fluorescence and minimal cell death. With this reagent, we observed a high rate of transfection and relatively healthy cells, indicating a high rate of retroviral packaging of nsp5-D4 for delivery into lymphoma cells. We believe that the lipid-based structure of the TransFectin was less toxic to the GP2-293 cells when compared to the chemicals in jetOPTIMUS and PEI which would contribute to the increased toxicity. Interestingly, other researchers have found that transfection with PEI and jetOPTIMUS can lead to high transfection rates, with jetOPTIMUS transfections also causing lower cell viability, although this was performed with HEK-293 cells from which GP2-293 cells are derived (Porosk et al., 2022).

Unsuccessful transfections with polymer-based transfection reagents could be explained by factors such as pH or molecular weight which only affect polymer-based transfection

reagents. It is also possible that lipid-based transfection reagents work better for GP2-293 cells. Cytotoxicity, as observed in Polyplus jetOPTIMUS transfections, is a frequently cited disadvantage to polymer-based transfection reagents, primarily due to the high charge density of these polymers. Low transfection efficiency when using PEI could be a result of human error on our behalf.

### **Retroviral Titration**

The Venus-C1 gene in each vector encodes the green fluorescent protein (GFP) which can be visualized in the GP2-293 cell line if the vector has successfully been introduced into the cells. In each of the transfections with the empty pLNCX2-VenusC1 vector and the pLNCX2-VenusC1-nsp5-D4 vector, green fluorescence can be clearly seen in the cells. This was only qualitatively assessed by the human eye to estimate the percentage of cells that were transfected. In these results, around a percentage of 50-80% transfection efficiency can be deduced.

To quantitatively measure the retrovirus yield, RT-qPCR was run to compare the relative success rate of transfection. The RT-qPCR results show the retrovirus yields by comparing their Cq values with the standard curve. However, we also recognized that our calculated Cq values of the unknown RNA concentrations showed some degree of error. In order to explore this slight deviance from our expectations, we completed a control RT-qPCR that assessed the clarity of the water used for the experiment, and we found that general water contamination could possibly account for these deviations.

### **Transduction**

Lastly, transduction was done using the recombinant retroviruses and the lymphoma cell line. It can be seen that the cells were transduced due to the presence of green fluorescence. The

rate of transduction was observed to be lower for the D4 retrovirus. A few reasons could have contributed to this low transduction efficiency. One reason would be that the timing to collect the transduced BCBL-1 samples was suboptimal. Another reason could be that expression levels were lower due to the insertion of the D4 gene in the plasmid. The transduction photos show that the packaging efficiency for the D4 vector is lower than that of the empty control vector. The transfection success directly correlates with the success of subsequent transductions, as the number of recombinant retroviruses determines the number of cells that can be infected. The supernatant from transfection with the D4 plasmid likely had a lower retroviral titer than the empty vector plasmid, which contributed to a lower transduction rate. The transduction efficiency was therefore slightly improved when concentrated supernatant was utilized. However, this improvement was still lower than expected. Potentially, this may have been due to the long incubation with the concentrating reagent and the supernatant which could have led to reduced retroviral viability.

### **Western Blotting Detection of STAT3**

The use of concentrated supernatant in transduction yielded a high enough transfection efficiency to enable GFP detection in western blot samples. The detection of GFP in the BCBL-1 samples directly indicates that the recombinant retroviruses were present in the BCBL-1 cells. Furthermore, GFP detection reveals that the nsp5-D4 sequence was ultimately integrated into the BCBL-1 cell genome for the experimental group. Both the control group (with the empty vector) and the experimental group both exhibited detectable GFP levels. GAPDH levels were used to normalize the STAT3 levels between the two samples and revealed a 37 percent decrease in STAT3 by nsp5-D4. This result is supported by the previous publications which describe the

degradational impact of nsp5 on STAT3. It is known that this effect is caused by nsp5-D4 because the nsp5-D4 sequence is the only difference between the control and testing plasmids.

### **Cell Viability Assay**

Transduction of BCBL-1 cells directly with nsp5-D4 retroviral supernatant from GP2-293 cells reduced cell number by 6-12% in comparison to cells transduced with the empty vector control. This decrease in cell number is likely due to the decrease of STAT3 in cells exposed to nsp5-D4. STAT3, as previously discussed, is ardently involved in the JAK-STAT pathway, which has strong impacts on cell growth and cell proliferation. Here, a result is observed that suggests that cell proliferation is successfully limited by the nsp5-D4 plasmid. When this result is taken in conjunction with the above western blot results, it becomes evident that the decrease in cell viability of the nsp5-D4 transduced cells is likely driven by the decrease in STAT3. However, until the molecular mechanism that drives this outcome is elucidated, it cannot be proven that this is the exact relationship. The best way to further confirm the relationship between nsp5-D4 and its effects on STAT3 are to conduct the *in vitro* studies with a mutant nsp5-D4. Additionally, the reduction of STAT3 and BCBL-1 cell number can be increased by transducing more retroviruses.

### **Limitations**

One limitation of this study is that retroviral delivery was not fully optimized, making it difficult to make conclusions about the impact of STAT3 on the cell viability of BCBL-1 cells. Due to time constraints, we were only able to start the final analysis of the nsp5-D4 effect on STAT3 and cell viability in BCBL-1 cells. Most of our time was spent performing and adjusting

the procedures for plasmid construction and transfection. For transduction, Western blotting and qRT-PCR, time constraints became a major issue.

Our main issue with transduction was the low fluorescence rate with the nsp5-D4 vector. With the empty vector, we were able to obtain much higher fluorescence. Optimization of the nsp5-D4 vector was restricted by time which forced us to move on in order to obtain Western blot results. Additionally, it was difficult to keep our BCBL-1 cells consistently healthy throughout the duration of the transduction. The cells would hover around being 50%-70% alive instead of 90%-100% alive. Without more time to improve cell health before running a transduction, our transduction efficiency was negatively impacted.

For Western blot, we began familiarizing ourselves with the procedure within the last month of the project due to unsatisfactory BCBL-1 transduction fluorescence, and therefore had limited time to perfect the procedure. Western blot is a time-consuming experiment with several hour waiting periods and often takes two days to complete. We also ran into more technical complications during the process. Our early runs of Western blot did not show any GAPDH or GFP expression due to issues of running buffers, primary antibodies, transfer, or some combination of the three. Ultimately, we were unable to reproduce the Western blot results due to time constraints. Since the only Western blot was successfully run, statistical analysis could not be performed to determine the significance of the results.

In addition to the time constraints, we were unable to conduct more qRT-PCR runs because of a lack of supplies. After running the procedure 3-4 times, our reagent materials ran out. Unfortunately, we were unable to get the correct supplies to obtain an ideal standard curve. Without adequate retroviral titer data, we were unable to draw a conclusion on the correlation

between the amount of viruses and transduction efficiency in a controlled number of BCBL-1 cells.

## Relevance

The STAT3 protein has many functions within the body, including partaking in immune responses (Arshad et al., 2020). Consequently, it has been the target of several forms of viral therapies, including nsp5 as tested in this research. Gene manipulation in STAT3 can also be significant for its influence on tumorigenesis in various cancer types. In one study, the genetic manipulation of STAT3 impacted the PKM2/SNAP23 pathway, which is involved in exosome biosynthesis. Furthermore, underexpression or overexpression of STAT3 in C26 colon cancer cells leads to worsened cachexia, a symptom of cancer (Fan et al., 2022).

The use of retroviral gene delivery systems has been successful in many *in vitro* and *in vivo* gene therapy experiments (Bulcha et al., 2021). Given the heterogeneous nature of this protein, our optimization of this system for delivery of nsp5 is therefore important to achieve successful treatment levels.

In theory, decreased levels of STAT3 proteins should be seen, leading to the downregulation of the effects of cytokines and growth factors that are involved in cancer cell proliferation, growth, and survival. Recent studies have shown that decreasing STAT3 levels through small molecule inhibitors can induce lymphoma cell death (Bai et al., 2019, Li et al., 2020). The findings of this research provide a starting point for analyzing the impact of nsp5 on STAT3 and the subsequent effects on BCBL-1 lymphoma cells. This insight, especially how nsp5 downregulates STAT3 and cancer cell growth, can advance treatment options for cancer in the future. Current drugs in clinical trials, such as dimethyl fumarate (DMF) produce antitumor effects in diffuse large B-cell lymphoma (DLBCL) but are not a targeted approach—it inhibits

JAK proteins (Schmitt et al., 2021). Another example is the JAK2 inhibitor TG101209, which inhibits Burkitt lymphoma cell growth (Zhang et al., 2021).

### **Future Directions**

As the impact of nsp5-D4 on STAT3 has been detected via Western blot analysis, further optimization of the Western blot procedure needs to be run to increase the strength of the results. Adjusting the volumes of the samples used in the Western blot to enable equal delivery of the amount of proteins would enable better comparison of STAT3 and GFP levels. An enzyme-linked immunosorbent assay (ELISA) could also be run to more easily quantify the amount of STAT3. From there, the next logical step is to examine the precise molecular mechanism of STAT3 degradation by nsp5 to understand why this effect is observed. If a mechanism is clarified, it would provide valuable insights into the precise role of STAT3 in the JAK/STAT pathway. That information could be utilized to better understand the molecular basis of protein signaling in cell proliferation. Since cancer is characterized by uncontrolled cell proliferation, a more comprehensive understanding of proliferative mechanisms opens the door to the creation of other treatments.

In the long term, we hope to study target specificity (degrading STAT3 versus other STAT proteins) and the effects of combination therapies. For combination therapies, we would test the effect of nsp5 therapy in combination with other drugs. One drug that seems to have promising synergistic effects on lymphoma is doxorubicin (Schmitt et al., 2021, Zhang et al., 2021). Future studies can combine nsp5 therapy with doxorubicin to see how the interactions of the two treatments impact lymphoma cancer cell viability.

## Chapter 6. Conclusions

The purpose of this research was to develop a molecular inhibitor for STAT3, which is a transcription factor that is upregulated in many types of cancers, including lymphoma, thus making it a therapeutic target of interest (Bai et al., 2019, Bharadwaj et al., 2014, La Sala et al., 2020, Li et al., 2020, Lu et al., 2016, Qi et al., 2020, Zhu et al., 2019). It has already been determined that the nsp5 viral protein, from PRRSV, can reduce STAT3 (Yang et al., 2017). By applying the nsp5 viral protein to lymphoma cells, we expected that nsp5 is able to inhibit cell proliferation and induce apoptosis by downregulating the STAT3 pathway. Degrading STAT3 seems to be the most promising option for reducing STAT3, since targeting various STAT3 domains at the gene and mRNA levels have issues with efficacy, specificity, or off-target toxicity (Bai et al., 2019, Chai et al., 2016, Huang et al., 2014, La Sala et al., 2020, Mishra et al., 2021, Son et al., 2017).

In this study, we provide results on the construction of an nsp5-D4 plasmid that can be packaged into retrovirus and delivered to lymphoma cells. This was done by restriction cloning, transfection into GP2-293 packaging cells, and transduction into BCBL-1 lymphoma cells. The impact of nsp5-D4 on BCBL-1 cells was then assessed by Western blot analysis and a cell viability assay. Our research indicates that STAT3 is reduced by nsp5-D4, and that the nsp5 protein also decreases BCBL-1 cell viability.

By conducting work on nsp5, which has been shown to inhibit the STAT3 pathway, we are contributing towards the body of research working on STAT3 inhibitors. The use of viral proteins is an emerging field in cancer treatment. This is the first study to use nsp5 as a STAT3 protein inhibitor for cancer treatment. Our investigation into this method of treatment will lead to a better understanding of whether nsp5 is adequate to treat lymphoma. Because this viral protein

reduced tumor cell growth *in vitro*, this is a promising step for developing a novel STAT3 inhibitor treatment that can then be assessed *in vivo* and potentially pass the preclinical development stage.

### References

Aigner, P., Mizutani, T., Horvath, J., Eder, T., Heber, S., Lind, K., Just, V., Moll, H. P., Yeroslaviz, A., Fischer, M., Kenner, L., Györfy, B., Sill, H., Grebien, F., Moriggl, R., Casanova, E., & Stoiber, D. (2019). STAT3 $\beta$  is a tumor suppressor in acute myeloid leukemia. *Blood Advances*, 3(13), 1989–2002.

<https://doi.org/10.1182/bloodadvances.2018026385>

Alberts, B., Johnson, A., Lewis, J., Morgan, D., Raff, M., Roberts, K., & Walter, P. (2015). Protein function. In Sherry Granum S.G. Lewis, & E. Zayatz (Eds.), *Molecular biology of the cell* (6th ed., pp.158-159). New York, NY: Garland Science.

American Cancer Society. (2023, January 12). *Key statistics for non-hodgkin lymphoma*.

American Cancer Society. <https://www.cancer.org/cancer/non-hodgkin-lymphoma/about/key-statistics.html>

Arshad, S., Naveed, M., Ullia, M., Javed, K., Butt, A., Khawar, M., & Amjad, F. (2020). Targeting STAT-3 signaling pathway in cancer for development of novel drugs:

Advancements and challenges. *Genetics and Molecular Biology*, 43.

<https://doi.org/10.1590/1678-4685-GMB-2018-0160>

Bai, L., Zhou, H., Xu, R., Zhao, Y., Chinnaswamy, K., McEachern, D., Chen, J., Yang, C. Y., Liu, Z., Wang, M., Liu, L., Jiang, H., Wen, B., Kumar, P., Meagher, J. L., Sun, D., Stuckey, J. A., & Wang, S. (2019). A potent and selective small-molecule degrader of STAT3 achieves complete tumor regression *In Vivo*. *Cancer cell*, 36(5), 498–511.e17.

<https://doi.org/10.1016/j.ccell.2019.10.002>

Berry, G. E., & Asokan, A. (2016). Cellular transduction mechanisms of adeno-associated viral vectors. *Current Opinion in Virology*, 21, 54–60.

<https://doi.org/10.1016/j.coviro.2016.08.001>

Bharadwaj, U., Kasembeli, M., Eckols, T., Kolosov, M., Lang, P., Christensen, K., Edwards, D., & Twardy, D. (2014). Monoclonal antibodies specific for STAT3 $\beta$  reveal its contribution to constitutive STAT3 phosphorylation in breast cancer. *Cancers*, 6(4), 2012–2034. <https://doi.org/10.3390/cancers6042012>

Bulcha, J. T., Wang, Y., Ma, H., Tai, P., & Gao, G. (2021). Viral vector platforms within the gene therapy landscape. *Signal Transduction and Targeted Therapy*, 6(1), 53.

<https://doi.org/10.1038/s41392-021-00487-6>

Carpenter, R., & Lo, H.-W. (2014). STAT3 target genes relevant to human cancers. *Cancers*, 6(2), 897–925. <https://doi.org/10.3390/cancers6020897>

Centers for Disease Control and Prevention. (2022, June 9). *Side effects of cancer treatment*. Centers for Disease Control and Prevention.

<https://www.cdc.gov/cancer/survivors/patients/side-effects-of-treatment.htm>

Chai, E. Z. P., Shanmugam, M. K., Arfuso, F., Dharmarajan, A., Wang, C., Kumar, A. P., Samy, R. P., Lim, L. H. K., Wang, L., Goh, B. C., Ahn, K. S., Hui, K. M., & Sethi, G. (2016). Targeting transcription factor STAT3 for cancer prevention and therapy.

*Pharmacology & Therapeutics*, 162, 86–97.

<https://doi.org/10.1016/j.pharmthera.2015.10.004>

Chalikonda, G., Lee, H., Sheik, A. *et al.* Targeting key transcriptional factor STAT3 in colorectal cancer. *Molecular Cellular Biochemistry* 476, 3219–3228 (2021).

<https://doi.org/10.1007/s11010-021-04156-8>

Challis, R. C., Ravindra Kumar, S., Chan, K. Y., Challis, C., Beadle, K., Jang, M. J., Kim, H. M., Rajendran, P. S., Tompkins, J. D., Shivkumar, K., Deverman, B. E., & Gradinaru, V. (2019). Systemic AAV vectors for widespread and targeted gene delivery in rodents. *Nature Protocols*, 14(2), 379–414. <https://doi.org/10.1038/s41596-018-0097-3>

Chnaiderman, J., Barro, M., & Spencer, E. (2002). Nsp5 phosphorylation regulates the fate of viral mRNA in rotavirus infected cells. *Archives of Virology*, 147(10), 1899–1911.

<https://doi.org/10.1007/s00705-002-0856-9>

Chang, K., Wang, T., & Luo, G. (2009). Proteomics study of the hepatitis C virus replication complex. In H. Tang (Ed.), *Hepatitis C: Methods and protocols* (pp. 185–193). Humana Press.

[https://doi.org/10.1007/978-1-59745-394-3\\_14](https://doi.org/10.1007/978-1-59745-394-3_14)

Clontech Laboratories, Inc. (n.d.). *Retroviral gene transfer and expression user manual*.

31. <https://www.takara.co.kr/file/manual/pdf/632508.pdf>

Creative Reaction Lab. (2018). *Equity-centered community design field guide*. St. Louis,

MO. <https://www.creativereactionlab.com/our-approach>

de Araujo, E. D., Keserü, G. M., Gunning, P. T., & Moriggl, R. (2020). Targeting STAT3

and STAT5 in cancer. *Cancers*, 12(8), 2002. <https://doi.org/10.3390/cancers12082002>

Fan, M., Sun, W., Gu, X., Lu, S., Shen, Q., Liu, X., & Zhang, X. (2022). The critical role of STAT3 in biogenesis of tumor-derived exosomes with potency of inducing cancer cachexia in vitro and in vivo. *Oncogene*, 41(7), 1050–1062.

<https://doi.org/10.1038/s41388-021-02151-3>

Fan, T. F., Bu, L. L., Wang, W. M., Ma, S. R., Liu, J. F., Deng, W. W., Mao, L., Yu, G. T., Huang, C. F., Liu, B., Zhang, W. F., & Sun, Z. J. (2015). Tumor growth suppression by inhibiting both autophagy and STAT3 signaling in HNSCC. *Oncotarget*, 6(41), 43581–43593. <https://doi.org/10.18632/oncotarget.6294>

Garcia-Reyero, J., Martinez Magunacelaya, N., Gonzalez de Villambrosia, S., Loghavi, S., Gomez Mediavilla, A., Tonda, R., Beltran, S., Gut, M., Pereña Gonzalez, A., d'Ámore, E., Visco, C., Khoury, J. D., & Montes-Moreno, S. (2021). Genetic lesions in MYC and STAT3 drive oncogenic transcription factor overexpression in plasmablastic lymphoma. *Haematologica*, 106(4), 1120–1128.

<https://doi.org/10.3324/haematol.2020.251579>

Greber, U. F., & Gomez-Gonzalez, A. (2021). Adenovirus: A blueprint for gene delivery. *Current Opinion in Virology*, 48, 49–56. <https://doi.org/10.1016/j.coviro.2021.03.006>

Groot, J. de, Ott, M., Wei, J., Kassab, C., Fang, D., Najem, H., O'Brien, B., Weathers, S.-P., Matsouka, C. K., Majd, N. K., Harrison, R. A., Fuller, G. N., Huse, J. T., Long, J. P., Sawaya, R., Rao, G., MacDonald, T. J., Priebe, W., DeCuypere, M., & Heimberger, A. B. (2022). A first-in-human phase I trial of the oral P-STAT3 inhibitor WP1066 in patients with recurrent malignant glioma. *CNS Oncology*, 11(02). <https://doi.org/10.2217/cns-2022-0005>

Hacker, U. T., Bentler, M., Kaniowska, D., Morgan, M., & Büning, H. (2020). Towards clinical implementation of adeno-associated virus (AAV) vectors for cancer gene therapy: Current status and future perspectives. *Cancers*, *12*(7), 1889.

<https://doi.org/10.3390/cancers12071889>

Hanahan, D. (2022). Hallmarks of cancer: New dimensions. *Cancer Discovery*, *12*(1), 31–46. <https://doi.org/10.1158/2159-8290.cd-21-1059>

Hu, G., Witzig, T. E., & Gupta, M. (2013). A novel missense (M206K) STAT3 mutation in diffuse large B cell lymphoma deregulates STAT3 signaling. *PLoS One*, *8*(7), e67851.

<https://doi.org/10.1371/journal.pone.0067851>

Hu, Y., Ke, P., Gao, P., Zhang, Y., Zhou, L., Ge, X., Guo, X., Han, J., & Yang, H.

(2021). Identification of an Intramolecular switch that controls the interaction of helicase nsp10 with membrane-associated nsp12 of porcine reproductive and respiratory syndrome virus. *Journal of Virology*, *95*(17), e0051821.

<https://doi.org/10.1128/JVI.00518-21>

Huang, W., Dong, Z., Wang, F., Peng, H., Liu, J.-Y., & Zhang, J.-T. (2014). A small molecule compound targeting STAT3 DNA-binding domain inhibits cancer cell proliferation, migration, and invasion. *ACS Chemical Biology*, *9*(5), 1188–1196.

<https://doi.org/10.1021/cb500071v>

Jonker, D. J., Nott, L., Yoshino, T., Gill, S., Shapiro, J., Ohtsu, A., Zalcborg, J., Vickers, M. M., Wei, A. C., Gao, Y., Tebbutt, N. C., Markman, B., Price, T., Esaki, T., Koski, S., Hitron, M., Li, W., Li, Y., Magoski, N. M., O'Callaghan, C. J. (2018). Napabucasin versus placebo in refractory advanced colorectal cancer: A randomised phase 3 trial. *The*

*Lancet Gastroenterology & Hepatology*, 3(4), 263–270. [https://doi.org/10.1016/s2468-1253\(18\)30009-8](https://doi.org/10.1016/s2468-1253(18)30009-8)

Kaczmarczyk, S. J., Sitaraman, K., Young, H. A., Hughes, S. H., & Chatterjee, D. K. (2011). Protein delivery using engineered virus-like particles. *Proceedings of the National Academy of Sciences*, 108(41), 16998–17003.

<https://doi.org/10.1073/pnas.1101874108>

Lara-Puente, J. H., Carreño, J. M., Sun, W., Suárez-Martínez, A., Ramírez-Martínez, L., Quezada-Monroy, F., Paz-De la Rosa, G., Viguera-Moreno, R., Singh, G., Rojas-Martínez, O., Chagoya-Cortés, H. E., Sarfati-Mizrahi, D., Soto-Priante, E., López-Macías, C., Krammer, F., Castro-Peralta, F., Palese, P., García-Sastre, A., & Lozano-Dubernard, B. (2021). Safety and immunogenicity of a newcastle disease virus vector-based SARS-CoV-2 vaccine candidate, AVX/COVID-12-HEXAPRO (Patria), in pigs. *mBio*, 12(5), e0190821. <https://doi.org/10.1128/mBio.01908-21>

La Sala, G., Michiels, C., Kükenshöner, T., Brandstoetter, T., Maurer, B., Koide, A., Lau, K., Pojer, F., Koide, S., Sexl, V., Dumoutier, L., & Hantschel, O. (2020). Selective inhibition of STAT3 signaling using monobodies targeting the coiled-coil and N-terminal domains. *Nature Communications*, 11(1), 4115. <https://doi.org/10.1038/s41467-020-17920-z>

Lee, H., & Ye, A. J. J. & S.-K. (2019). Highlighted STAT3 as a potential drug target for cancer therapy. *BMB Reports*, 52(7), 415–423.

<https://doi.org/10.5483/BMBRep.2019.52.7.152>

Larionova, I., Kazakova, E., Patysheva, M., & Kzhyshkowska, J. (2020). Transcriptional, epigenetic and metabolic programming of tumor-associated macrophages. *Cancers*,

12(6). <https://doi.org/10.3390/cancers12061411>

Li, Y., Tas, A., Sun, Z., Snijder, E. J., & Fang, Y. (2015). Proteolytic processing of the porcine reproductive and respiratory syndrome virus replicase. *Virus Research*, 202, 48–59. <https://doi.org/10.1016/j.virusres.2014.12.027>

Li, X., Wei, Y., & Wei, X. (2020). Napabucasin, a novel inhibitor of STAT3, inhibits growth and synergises with doxorubicin in diffuse large B-cell lymphoma. *Cancer Letters*, 491, 146–161. <https://doi.org/10.1016/j.canlet.2020.07.032>

Liu, Y., Liao, S., Bennett, S., Tang, H., Song, D., Wood, D., Zhan, X., & Xu, J. (2021). STAT3 and its targeting inhibitors in osteosarcoma. *Cell Proliferation*, 54(2), e12974. <https://doi.org/10.1111/cpr.12974>

Lü, Z., Li, X., Li, K., Wang, C., Du, T., Huang, W., Ji, M., Li, C., Xu, F., Xu, P., & Niu, Y. (2021). Structure-activity study of nitazoxanide derivatives as novel STAT3 pathway inhibitors. *ACS Medicinal Chemistry Letters*, 12(5), 696–703. <https://doi.org/10.1021/acsmchemlett.0c00544>

Lu, Y., Chen, W., Zhu, Chen, J., Chen, W., Chen, N. (2016). Eriocalyxin B blocks human SW1116 colon cancer cell proliferation, migration, invasion, cell cycle progression and angiogenesis via the JAK2/stat3 signaling pathway. *Molecular Medicine Reports*, 13(3), 2235–2240. <https://doi.org/10.3892/mmr.2016.4800>

Lukashev, A. N., & Zamyatnin, A. A. (2016). Viral vectors for gene therapy: Current state and clinical perspectives. *Biochemistry Moscow*, 81(7), 700–708. <https://doi.org/10.1134/S0006297916070063>

Maetzig, T., Baum, C., & Schambach, A. (2012). Retroviral protein transfer: Falling apart to make an impact. *Current Gene Therapy*, 12(5), 389–409.

<https://doi.org/10.2174/156652312802762581>

Manocha, E., Caruso, A., & Caccuri, F. (2021). Viral Proteins as Emerging Cancer Therapeutics. *Cancers*, *13*(9), 2199. <https://doi.org/10.3390/cancers13092199>

Mariotto, A. B., Enewold, L., Zhao, J., Zeruto, C. A., & Yabroff, K. R. (2020). Medical care costs associated with cancer survivorship in the United States. *Cancer Epidemiology, Biomarkers & Prevention*, *29*(7), 1304–1312.

<https://doi.org/10.1158/1055-9965.epi-19-1534>

Medina-Kauwe, L. K. (2013). Development of adenovirus capsid proteins for targeted therapeutic delivery. *Therapeutic Delivery*, *4*(2), 267–277.

<https://doi.org/10.4155/tde.12.155>

Mertens, C., Haripal, B., Klinge, S., & J.E., Darnell. (2015). Mutations in the linker domain affect phospho-STAT3 function and suggest targets for interrupting STAT3 activity. *Proceedings of the National Academy of Sciences of the United States of America*, *112*(48), 14811-14817. doi: <https://10.1073/pnas>.

Miller A. D. (2014). Retroviral vectors: from cancer viruses to therapeutic tools. *Human Gene Therapy*, *25*(12), 989–994. <https://doi.org/10.1089/hum.2014.2542>

Mishra, S., Kumar, S., Choudhuri, K., Longkumer, I., Koyyada, P., & Kharsyiemiong, E. T. (2021). Structural exploration with AlphaFold2-generated STAT3 $\alpha$  structure reveals selective elements in STAT3 $\alpha$ -GRIM-19 interactions involved in negative regulation. *Scientific Reports*, *11*(1), 23145. <https://doi.org/10.1038/s41598-021-01436-7>

Nan, H., Lan, J., Tian, M., Dong, S., Tian, J., Liu, L., Xu, X., & Chen, H. (2018). The network of interactions among porcine reproductive and respiratory syndrome virus non-

structural proteins. *Frontiers in Microbiology*, 9, 970.

<https://doi.org/10.3389/fmicb.2018.00970>

National Cancer Institute. (2013). *Newcastle Disease Virus (PDQ)-Patient Version*. U.S. Department of Health and Human Services, National Institutes of Health.

<https://www.cancer.gov/about-cancer/treatment/cam/patient/ndv-pd>

National Cancer Institute. (2019, May 16). *Symptoms of cancer?*. U.S. Department of Health and Human Services, National Institutes of Health. <https://www.cancer.gov/about-cancer/diagnosis-staging/symptoms>

National Cancer Institute. (2020, September 25). *Cancer statistics*. U.S. Department of Health and Human Services, National Institutes of Health. <https://www.cancer.gov/about-cancer/understanding/statistics>

National Cancer Institute. (2021, October 11). *What is cancer?*. U.S. Department of Health and Human Services, National Institutes of Health. <https://www.cancer.gov/about-cancer/understanding/what-is-cancer>

National Cancer Institute. (2022a, October 14). *Cancer staging*. U.S. Department of Health and Human Services, National Institutes of Health. <https://www.cancer.gov/about-cancer/diagnosis-staging/staging>

National Cancer Institute. (2022b, December 22). *Adult hodgkin lymphoma treatment (PDQ)-Patient version*. U.S. Department of Health and Human Services, National Institutes of Health. [https://www.cancer.gov/types/lymphoma/patient/adult-hodgkin-treatment-pdq#\\_57](https://www.cancer.gov/types/lymphoma/patient/adult-hodgkin-treatment-pdq#_57)

National Cancer Institute. (2022c, December 29). *Adult non-hodgkin lymphoma treatment (PDQ)-Patient version*. U.S. Department of Health and Human Services, National Institutes of Health. <https://www.cancer.gov/types/lymphoma/patient/adult-nhl-treatment-pdq>

O’Keefe, E. P. (2021). Nucleic acid delivery: lentiviral and retroviral vectors. *Materials and Methods*, 3, 174. <https://www.labome.com/method/Nucleic-Acid-Delivery-Lentiviral-and-Retroviral-Vectors.html>

Porosk, L., Nebogatova, J., Härk, H. H., Vunk, B., Arukuusk, P., Toots, U., Ustav, M., Langel, Ü., & Kurrikoff, K. (2022). Predicting transiently expressed protein yields: comparison of transfection methods in CHO and HEK293. *Pharmaceutics*, 14(9), 1949. <https://doi.org/10.3390/pharmaceutics14091949>

Proia, T. A., Singh, M., Woessner, R., Carnevalli, L., Bommakanti, G., Magiera, L., Srinivasan, S., Grosskurth, S., Collins, M., Womack, C., Griffin, M., Ye, M., Cantin, S., Russell, D., Xie, M., Hughes, A., Deng, N., Mele, D. A., Fawell, S., ... McCoon, P. (2020). STAT3 antisense oligonucleotide remodels the suppressive tumor microenvironment to enhance immune activation in combination with anti-PD-L1. *Clinical Cancer Research*, 26(23), 6335–6349. <https://doi.org/10.1158/1078-0432.ccr-20-1066>

Promega Corporation. (2015). *Luciferase Assay System*. Promega. <https://www.promega.com/Products/luciferase-assays/Reporter-Assays/Luciferase-AssaySystem/?catNum=E1500>

Roca Suarez, A. A., Van Renne, N., Baumert, T. F., & Lupberger, J. (2018). Viral

manipulation of STAT3: Evade, exploit, and injure. *PLoS Pathogens*, 14(3).

<https://doi.org/10.1371/journal.ppat.1006839>

Qi, X., Li, M., Zhang, X.-min, Dai, X.-fen, Cui, J., Li, D.-hai, Gu, Q.-qun, Lv, Z.-hua, & Li, J. (2020). Trichothecin inhibits cancer-related features in colorectal cancer development by targeting STAT3. *Molecules*, 25(10), 2306. <https://doi.org/10.3390/molecules25102306>

Rascón-Castelo, E., Burgara-Estrella, A., Mateu, E., & Hernández, J. (2015).

Immunological features of the non-structural proteins of porcine reproductive and respiratory syndrome virus. *Viruses*, 7(3), 873–886. <https://doi.org/10.3390/v7030873>

Sahoo, S., Kariya, T., & Ishikawa, K. (2021). Targeted delivery of therapeutic agents to the heart. *Nature reviews. Cardiology*, 18(6), 389–399. <https://doi.org/10.1038/s41569-020-00499-9>

Sánchez, D., Pelayo, R., Medina, L. A., Vadillo, E., Sánchez, R., Núñez, L., Cesarman-Maus, G., & Sarmiento-Silva, R. E. (2016). Newcastle disease virus: Potential therapeutic application for human and canine lymphoma. *Viruses*, 8(1), 3.

<https://doi.org/10.3390/v8010003>

Santiago-Ortiz, J. L., & Schaffer, D. V. (2016). Adeno-associated virus (AAV) vectors in cancer gene therapy. *Journal of Controlled Release*, 240, 287–301.

<https://doi.org/10.1016/j.jconrel.2016.01.001>

Schmitt, A., Xu, W., Bucher, P., Grimm, M., Konantz, M., Horn, H., Zapukhlyak, M., Berning, P., Brändle, M., Jarboui, M.-A., Schönfeld, C., Boldt, K., Rosenwald, A., Ott, G., Grau, M., Klener, P., Vockova, P., Lengerke, C., Lenz, G., ... Hailfinger, S. (2021).

Dimethyl fumarate induces ferroptosis and impairs NF-KB/STAT3 signaling in DLBCL. *Blood*, 138(10), 871–884. <https://doi.org/10.1182/blood.2020009404>

Sever, R., & Brugge, J. S. (2015). Signal transduction in cancer. *Cold Spring Harbor Perspectives in Medicine*, 5(4). <https://doi.org/10.1101/cshperspect.a006098>

Seyfried, T. N., & Huysentruyt, L. C. (2013). On the origin of cancer metastasis. *Critical Reviews in Oncogenesis*, 18(1-2), 43-73. <https://doi.org/10.1615/critrevoncog.v18.i1-2.40>

Shamir, I., Abutbul-Amitai, M., Abbas-Egbariya, H., Pasmanik-Chor, M., Paret, G., & Nevo-Caspi, Y. (2020). STAT3 isoforms differentially affect ACE2 expression: A potential target for COVID-19 therapy. *Journal of Cellular and Molecular Medicine*, 24(21), 12864–12868. <https://doi.org/10.1111/jcmm.15838>.

Shi, Y., Zhang, Z., Qu, X., Zhu, X., Zhao, L., Wei, R., Guo, Q., Sun, L., Yin, X., Zhang, Y., & Li, X. (2018). Roles of STAT3 in Leukemia (review). *International Journal of Oncology*, 53, 7-20. <https://doi.org/10.3892/ijo.2018.4386>

Shi, S., Ma, H. Y., & Zhang, Z. G. (2021). Clinicopathological and prognostic value of STAT3/p-STAT3 in cervical cancer: A meta and bioinformatics analysis. *Pathology, Research and Practice*, 227, 153624. <https://doi.org/10.1016/j.prp.2021.153624>

Siegel, R. L., Miller, K. D., Fuchs, H. E., & Jemal, A. (2022). Cancer statistics, 2022. *CA: A Cancer Journal for Clinicians*, 72(1), 7–33. <https://doi.org/10.3322/caac.21708>

Son, D. J., Zheng, J., Jung, Y. Y., Hwang, C. J., Lee, H. P., Woo, J. R., Baek, S. Y., Ham, Y. W., Kang, M. W., Shong, M., Kweon, G. R., Song, M. J., Jung, J. K., Han, S. B., Kim, B. Y., Yoon, D. Y., Choi, B. Y., & Hong, J. T. (2017). MMPP attenuates non-small cell

lung cancer growth by inhibiting the STAT3 DNA-binding activity via direct binding to the STAT3 DNA-binding domain. *Theranostics*, 7(18), 4632–4642.

<https://doi.org/10.7150/thno.18630>

Song, X., Liu, C., Wang, N., Huang, H., He, S., Gong, C., & Wei, Y. (2021). Delivery of CRISPR/Cas systems for cancer gene therapy and immunotherapy. *Advanced Drug Delivery Reviews*, 168, 158–180. <https://doi.org/10.1016/j.addr.2020.04.010>

Song, J., Li, K., Li, T., Zhao, G., Zhou, S., Li, H., Li, J., & Weng, C. (2020). Screening of PRRSV- and ASFV-encoded proteins involved in the inflammatory response using a porcine iGLuc reporter. *Journal of Virological Methods*, 285, 113958.

<https://doi.org/10.1016/j.jviromet.2020.113958>

Song, J., Liu, Y., Gao, P., Hu, Y., Chai, Y., Zhou, S., Kong, C., Zhou, L., Ge, X., Guo, X., Han, J., & Yang, H. (2018a). Mapping the nonstructural protein interaction network of porcine reproductive and respiratory syndrome virus. *Journal of Virology*, 92(24), e01112-18. <https://doi.org/10.1128/JVI.01112-18>

Song, T. L., Nairismägi, M. L., Laurensia, Y., Lim, J. Q., Tan, J., Li, Z. M., Pang, W. L., Kizhakeyil, A., Wijaya, G. C., Huang, D. C., Nagarajan, S., Chia, B. K., Cheah, D., Liu, Y. H., Zhang, F., Rao, H. L., Tang, T., Wong, E. K., Bei, J. X., Iqbal, J., Ong, C. K. (2018b). Oncogenic activation of the STAT3 pathway drives PD-L1 expression in natural killer/T-cell lymphoma. *Blood*, 132(11), 1146–1158. <https://doi.org/10.1182/blood-2018-01-829424>

Takara Bio USA. (n.d.). *Retro-X<sup>TM</sup> qRT-PCR Titration Kit User Manual*. 11. Cat. No.

631453 (050919). [https://www.takarabio.com/documents/User%20Manual/Retro/Retro-X%20qRT-PCR%20Titration%20Kit%20User%20Manual%20%28PT3952-1%29\\_050919.pdf](https://www.takarabio.com/documents/User%20Manual/Retro/Retro-X%20qRT-PCR%20Titration%20Kit%20User%20Manual%20%28PT3952-1%29_050919.pdf)

Tannous B. A. (2009). Gaussia luciferase reporter assay for monitoring biological processes in culture and in vivo. *Nature Protocols*, 4(4), 582–591.  
<https://doi.org/10.1038/nprot.2009.28>

Turton, K. B., Annis, D. S., Rui, L., Esnault, S., & Mosher, D. F. (2015). Ratios of four STAT3 splice variants in human eosinophils and diffuse large B cell lymphoma cells. *PLOS ONE*, 10(5), e0127243. <https://doi.org/10.1371/journal.pone.0127243>

ThermoFisher Scientific. (2009a). *Cell culture protocols*.  
<https://www.thermofisher.com/us/en/home/references/gibco-cell-culture-basics/cell-culture-protocols.html>

Vargas, J. E., Chicaybam, L., Stein, R. T., Tanuri, A., Delgado-Cañedo, A., & Bonamino, M. H. (2016). Retroviral vectors and transposons for stable gene therapy: Advances, current challenges and perspectives. *Journal of Translational Medicine*, 14(1), 288.  
<https://doi.org/10.1186/s12967-016-1047-x>

Vijayakumar, G., McCroskery, S., & Palese, P. (2020). Engineering Newcastle Disease Virus as an Oncolytic Vector for Intratumoral Delivery of Immune Checkpoint Inhibitors and Immunocytokines. *Journal of Virology*, 94(3), e01677-19.  
<https://doi.org/10.1128/JVI.01677-19>

Wang, J., Ke, Y., & Shu, T. (2020a). Crocin has pharmacological effects against the pathological behavior of colon cancer cells by interacting with the STAT3 signaling

pathway. *Experimental and Therapeutic Medicine*, 19(2), 1297–1303.

<https://doi.org/10.3892/etm.2019.8329>

Wang, L., Qin, W., Huo, Y. J., Li, X., Shi, Q., Rasko, J. E. J., Janin, A., & Zhao, W. L.

(2020b). Advances in targeted therapy for malignant lymphoma. *Signal Transduction and Targeted Therapy*, 5(1), 15. <https://doi.org/10.1038/s41392-020-0113-2>

Wei, N., Li, J., Fang, C., Chang, J., Xirou, V., Syrigos, N. K., Marks, B. J., Chu, E., &

Schmitz, J. C. (2019). Targeting colon cancer with the novel STAT3 inhibitor

bruceantinol. *Oncogene*, 38(10), 1676–1687. <https://doi.org/10.1038/s41388-018-0547-y>

Wyatt, J., Müller, M. M., & Tavassoli, M. (2019). Cancer treatment goes viral: using

viral proteins to induce tumour-specific cell death. *Cancers*, 11(12), 1975.

<https://doi.org/10.3390/cancers11121975>

World Health Organization. (2022, February 3). *Cancer*. World Health Organization.

<https://www.who.int/news-room/fact-sheets/detail/cancer>

Xiong, Y. J., Liu, D. Y., Shen, R. R., & Xiong, Y. (2021). A short deletion in the DNA-binding domain of STAT3 suppresses growth and progression of colon cancer cells.

*Aging*, 13(4), 5185–5196. <https://doi.org/10.18632/aging.202439>

Xu, X., Chen, W., Zhu, W., Chen, J., Ma, B., Ding, J., Wang, Z., Li, Y., Wang, Y., &

Zhang, X. (2021). Adeno-associated virus (aav)-based gene therapy for glioblastoma.

*Cancer Cell International*, 21(1). <https://doi.org/10.1186/s12935-021-01776-4>

Yang, L., Lin, S., Kang, Y., Xiang, Y., Xu, L., Li, J., Dai, X., Liang, G., Huang, X., &

Zhao, C. (2019). Rhein sensitizes human pancreatic cancer cells to EGFR inhibitors by

inhibiting STAT3 pathway. *Journal of Experimental & Clinical Cancer Research*, 38(1),

31. <https://doi.org/10.1186/s13046-018-1015-9>

- Yang, L., Lin, S., Xu, L., Lin, J., Zhao, C., & Huang, X. (2019). Novel activators and small-molecule inhibitors of STAT3 in cancer. *Cytokine & Growth Factor Reviews*, *49*, 10–22. <https://doi.org/10.1016/j.cytogfr.2019.10.005>
- Yang, L., Wang, R., Ma, Z., Xiao, Y., Nan, Y., Wang, Y., Lin, S., & Zhang, Y.-J. (2017). Porcine reproductive and respiratory syndrome virus antagonizes JAK/STAT3 signaling via nsp5, which induces STAT3 degradation. *Journal of Virology*, *91*(3). <https://doi.org/10.1128/JVI.02087-16>
- Yang, L., Wang, R., Ma, Z., Wang, Y., & Zhang, Y. (2015). Inducing Autophagic cell death by nsp5 of porcine reproductive and respiratory syndrome virus. *Austin Virology and Retro Virology*, *2*(2): 1014.
- Yu, X., He, L., Cao, P., & Yu, Q. (2015). Eriocalyxin B Inhibits STAT3 Signaling by Covalently Targeting STAT3 and Blocking Phosphorylation and Activation of STAT3. *PLOS ONE*, *10*(5), e0128406. <https://doi.org/10.1371/journal.pone.0128406>
- Zhang, X., Dong, W., Wang, X., Zhu, Z., He, S., Zhang, H., Chen, Y., Liu, X., & Guo, C. (2022). Exostosin glycosyltransferase 1 reduces porcine reproductive and respiratory syndrome virus infection through proteasomal degradation of nsp3 and nsp5. *Journal of Biological Chemistry*, *298*(2), 101548. <https://doi.org/10.1016/j.jbc.2021.101548>
- Zhang, Y., Li, J., Zhong, H., Xiao, X., Wang, Z., Cheng, Z., Hu, C., Zhang, G., & Liu, S. (2021). The JAK2 inhibitor TG101209 exhibits anti-tumor and chemotherapeutic sensitizing effects on Burkitt lymphoma cells by inhibiting the JAK2/STAT3/c-MYB signaling axis. *Cell Death Discovery*, *7*(1), 268. <https://doi.org/10.1038/s41420-021-00655-1>

Zhang, H.-X., Yang, P.-L., Li, E.-M., & Xu, L.-Y. (2019a). Stat3beta, a distinct isoform from stat3. *The International Journal of Biochemistry & Cell Biology*, *110*, 130–139.

<https://doi.org/10.1016/j.biocel.2019.02.006>

Zhang, W., Chen, K., Guo, Y., Chen, Y., & Liu, X. (2019b). Involvement of PRRSV NSP3 and NSP5 in the autophagy process. *Virology Journal*, *16*(1), 13.

<https://doi.org/10.1186/s12985-019-1116-x>

Zhao, Y., Liu, Z., Li, L., Wu, J., Zhang, H., Zhang, H., Lei, T., & Xu, B. (2021).

Oncolytic Adenovirus: Prospects for cancer immunotherapy. *Frontiers in Microbiology*, *12*. <https://doi.org/10.3389/fmicb.2021.707290>

Zhao, X., Zhang, Z., Moreira, D., Su, Y. L., Won, H., Adamus, T., Dong, Z., Liang, Y., Yin, H. H., Swiderski, P., Pillai, R. K., Kwak, L., Forman, S., & Kortylewski, M. (2018). B cell lymphoma immunotherapy using TLR9-targeted oligonucleotide STAT3

inhibitors. *Molecular Therapy*, *26*(3), 695–707.

<https://doi.org/10.1016/j.ymthe.2018.01.007>

Zheng, Z.-Y., Yang, P.-L., Li, R.-Y., Liu, L.-X., Xu, X.-E., Liao, L.-D., Li, X., Chu, M.-Y., Peng, L., Huang, Q.-F., Heng, J.-H., Wang, S.-H., Wu, Z.-Y., Chang, Z.-J., Li, E.-M., & Xu, L.-Y. (2021). STAT3 $\beta$  disrupted mitochondrial electron transport chain enhances chemosensitivity by inducing pyroptosis in esophageal squamous cell carcinoma. *Cancer Letters*, *522*, 171–183. <https://doi.org/10.1016/j.canlet.2021.09.035>

Zhu, F., Wang, K. B., & Rui, L. (2019). STAT3 activation and oncogenesis in lymphoma. *Cancers*, *12*(1), 19. <https://doi.org/10.3390/cancers12010019>

Zou, S., Tong, Q., Liu, B., Huang, W., Tian, Y., & Fu, X. (2020). Targeting STAT3 in cancer immunotherapy. *Molecular Cancer*, *19*(1). <https://doi.org/10.1186/s12943-020-01258-7>

## **Appendices**

### **Appendix A: PCR Amplification of Target Genes and Cloning**

In order to insert the PRRSV nsp5 gene into the pLNCX2 vector with the Venus tag, three PCRs must be performed. The first PCR will use the forward primer VenusC1-F-iXhoI while the reverse primer will be VenusC1-HL-R1 on the Venus gene sequence. Then, the second PCR will use the forward primer HL-nsp5-F2 which contains the XhoI restriction site and the

reverse primer 85nsp5-R22 which contains the HindIII restriction site on the nsp sequence. The third PCR will be an overlap PCR where the products from the first PCR and the second PCR form the template. In this last PCR, the primers which will be used are VenusC1-F-iXhoI and 85nsp5-R22. The product of these overall PCRs will be a recombinant molecule composed of the Venus tag and nsp5.

Next, the product from the third PCR will be cut with restriction enzymes BsmBI/HindIII. This will be ligated into the pLNCX2 transfer vector which has been cut by XhoI/HindIII. The sequencing primers for this recombinant vector are pLNCX2-F1 and pLNCX2-R1 and they can be used to ensure the vector contains the right sequence.

### **A.1 D4 Amplification**

1. Obtain primers and Master mix from Gemstone 2021 box in -20 degree freezer in PCR room
2. Aliquoted 1 mL of water into a microcentrifuge tube, labeled under PCR hood
3. Add the following to a flat cap PCR tube in the PCR room:
  - a. 25 uL 2X Phusion Flash High Fidelity PCR master mix
  - b. 2.5 uL F21 Primer
  - c. 2.5 uL R2 primer
  - d. 18 uL of aliquoted water
4. Go to main room and add the following to the PCR tube:
  - a. 2 uL of plasmid (PLXSN-HA-nsp5, or any other nsp5 plasmid)
5. Total Reaction system should be as follows:

	Volume
2X Phusion Flash High Fidelity PCR master mix	25 uL
Forward Primer	2.5 uL
Reverse Primer	2.5 uL
Template cDNA	2 uL
Nuclease-free water	18 uL
	50 uL

6. Put tube in PCR machine and run the following (PCR thermal cycling conditions):

Step	Temperature (°C)	Time	Number of cycles
Initial denaturation	98	10 s	1
Denaturation	98	1 s	30
Annealing	60	5 s	
Extension	72	15 s/ 1 kb	
Final Extension	72	5 min	1

7. Remove final PCR product and store in 4 °C or move to purification (Appendix A.2)

## **A.2 Purification of PCR product (Using GeneJET PCR purification kit)**

1. Take tube out of PCR machine
2. Add 1:1 ratio of binding buffer to PCR product
  - a. So if your PCR product is 50 uL, use 50 uL binding buffer
  - b. Spin down quickly to mix, should be yellow after mixing
3. Add all of sample to GeneJET column (100 uL in this example)
  - a. Can hold up to 800 uL solution
4. Centrifuge at 12,000 rpm for 1 min
5. Discard flow through
6. Add 700 uL wash buffer (from miniprep kit)
7. Repeat steps 4 and 5
8. Repeat step 4
9. Put blue tube into new microcentrifuge tube and add 50 uL of nuclease free water
  - a. put directly onto filter without touching anything
10. Repeat step 4
11. Throw away the blue tube and label the microcentrifuge tube (make sure to add 'purified', plasmid name, and date to the tube)
12. Store in 4 °C fridge

## **A.3 Checking DNA Concentration (using BioTek software)**

1. Get 96 well plate. Add 98 uL of water to 48 wells.
2. Put 96 well plate into BioTek sequencing machine. Open BioTek software on the computer.

3. Under the 'experiments' tab, select the DNA protocol (DNA-CONC1.prt). This should have it set as reading the plate for 4 wavelengths.
4. Once you enter experiment 1, expand the protocol tab
5. Click on 'plate layout'
6. For the wells that are filled with water, select the type 'sample' which is under 'well settings'.
  - a. You may have to clear the plate first
7. Once you highlighted the water wells with sample, select 'empty' for empty wells.
8. Click the 'read plate' button which is located next to the Com1 button
9. After the plate is read, find the same DNA260 for total # of samples + control
  - a. Ex: if I am trying to find the concentration of PLXSN-VenusC1-nsp5-D4 and PLNCX2-VenusC1-nsp5-D4, then I need 3 wells with the same DNA260 value- 2 for the samples, and 1 as a control
10. Add 2 uL of each plasmid (1 per well) then shake the plate gently
  - a. Do NOT place the plate on the cloth fiber- this could change the absorbance; put the plate on a sheet of paper when you add the plasmid
11. Reload the plate
12. Click 'plate layout' (same as step 5) and clear plate
13. Select the type as 'sample' and highlight which wells will be the sample (the ones with plasmid in them)
14. Select the type and 'blank' and highlight which well will be the blank (the control well)
15. Click 'read plate'

16. After you read plate and record concentration value (using 'conc' in the dropdown menu), write concentration on the plasmid tube, rinse plate with distilled water, and dap plate on a paper towel.
17. Wrap up plate and store for next use.

#### A.4 Sanger Sequencing

1. Perform calculations using DNA concentrations to figure out how much DNA to add. Then, figure out which primer to add. One PCR tube should contain the following:

<b>Materials</b>	<b>Sample (may have more samples)</b>
Buffer 5X	1.75 $\mu\text{L}$
Big Dye	0.50 $\mu\text{L}$
DNA (plasmid)	300-500 ng
Primer (one tube has forward primer, one tube has reverse primer; so 2 tubes per sample)	1 $\mu\text{L}$ of 1 $\mu\text{M}$
H <sub>2</sub> O	(add to fill total volume to 10 $\mu\text{L}$ - may not need)
<b>Total Volume</b>	10 $\mu\text{L}$

2. Go to the PCR room- take ice bucket. Primer, buffer, and big dye should be stored in -20 degree fridge. Take them out and leave on ice.
  - a. Change gloves/ put on the coat to avoid contamination
3. Collect the number of flat cap PCR tubes needed. Make sure to label tubes (number them) and write down which tube corresponds to what sample
  - a. make sure to add the concentration of the DNA that you use
4. Add appropriate aliquots of big dye and buffer to each tube. Then, add primer
  - a. record which primer went into which tube
5. Centrifuge tubes with big dye, buffer, and and primer
6. Put primers, big dye, and buffer back into fridge. Turn on UV light. Take PCR tubes to main room to add DNA
7. Add appropriate aliquot of DNA to each tube. Remember, there should be 2 tubes per DNA sample.
8. If tube is not yet at 10 uL, add appropriate aliquot of water.
9. Use the centrifuge to spin samples down
10. Put tubes in the sequencing machine
11. Turn on the sequencing machine. Check to make sure it matches the following:

Step	Temperature (°C)	Time	Number of cycles
Initial denaturation	96	10 s	1
Denaturation	95	1 s	25
Annealing	50	5 s	

Extension	60	15 s/ 1 kb	
Final Extension	25	5 min	1

12. Add 2.5 uL of 25 mM EDTA and 30 uL of 100% ethanol to 1.5 mL tubes (per sample- so 4 PCR tubes would mean add this amount to 4 tubes).
13. Transfer 10 uL PCR reaction mixture to 1.5 mL tube. Vortex and incubate (for 15 min or overnight)
14. Centrifuge for 30 min at 4 degree C
15. Remove supernatant
16. Add 30 uL of 70% ethanol to each tube
17. Repeat step 14
18. Remove supernatant carefully, dry pellet in dark 37 degree incubator for 1-2 minutes
19. Resuspend pellet in 10 uL Hi-Di buffer
20. Denature on 100 degree heat block (on bench in front of ours) for 5 min
21. Cool in ice bucket for 5 min
22. Load to sampler plate
  - a. Should be 10 uL in a 96- well plate (pipette all of sample into well)
23. Use 3130 Genetic Analyzer to run sequencing program. Check results in 3 hours.

### A.5 Double-Restriction Enzyme Digestion

1. Perform digestion using double restriction enzymes. Below are tables for sample restriction enzymes that can be used. Check the Thermo Fisher Scientific User manual for the enzymes for more specific information.
2. Label (2) 1.5mL eppendorf tubes with vector, digestion, date
3. Add the following digestion mixes into each tube
  - a. restriction enzyme amount depends on concentration. Make sure you check the concentration on the tube

Double-Restriction Digest on Plasmid:

10 X R Buffer	10 uL
Plasmid*	30 uL (need 3ug)
Hind III	1 uL if 100u/ul, 7.5ul if 10u/ul
Xho I	2.5 uL if 10u/ul
Nuclease-Free Water*	However much to make 50 uL
Total Volume:	50 uL

Double-Restriction Digest on Insert:

10 X R Buffer	10 uL
---------------	-------

Purified PCR Product (Insert)*	30 uL (need 3ug)
Hind III	1 uL if 100u/ul, 7.5ul if 10u/ul
Xho I	2.5 uL if 10u/ul
Nuclease-Free Water*	However much to make 50 uL
Total Volume:	50 uL

\*Note: Adjust volumes of plasmid and PCR product based on their concentrations to get 3 ug. If the plasmid or PCR product volumes are changed, then adjust the volume of nuclease-free water accordingly to get the correct total volume.

4. Quickly spin down
5. Incubated in 37 degree water bath for 2 hours or overnight
  - a. Make sure to wrap the top in parafilm, make sure no water enters
6. Purify the digested plasmid and digester PCR product with the GeneJet PCR Purification kit (protocol B.2)
7. Run a DNA gel on both digestion products to ensure complete digestion
8. Store in 4 degree fridge for ligation

### A.6 Ligation

1. Obtain purified and digested PCR product (nsp5-D4) and purified and digested plasmid (PLNCX2 vector)
  - a. Should be stored in 4 degree fridge or are located in 37 degree water bath
2. Calculate the amount of PCR product and vector needed based on concentration.

- a. If the amount needed surpasses 10 uL, then scale the procedure up so the reaction system is a total 15 uL volume (set up proportions to figure out amounts of ligase, buffer, and water needed)
- i. Ex:  $\frac{2 \text{ uL } 5X \text{ ligase buffer}}{10 \text{ uL reaction system}} = \frac{x \text{ uL } 5X \text{ ligase buffer}}{15 \text{ uL reaction system}}$
  - ii. This will change the chart used below to a total volume of 15 uL.
3. Prepare ligation mixture in a 1.5 mL tube (all materials should be on ice)

T4 ligase	0.5 uL
5X Ligase Buffer	2 uL
Digested/ Purified Vector (plasmid)	50 ng
Digested/ Purified PCR product (D4)	150 ng
Nuclease Free Water	add if total volume is NOT 10 uL
Total volume	10 uL

\*\*Note: if you have 10X Ligase Buffer, you add 1 uL

4. Incubate at room temp for 10 min
- a. If you use more T4 ligase (>0.5 uL), then increase incubation time proportionally

### **Transformation by Heat Shock**

5. Remove DH5 alpha/ E. coli from -80 degree freezer and thaw partially

6. When thawed, add total 10 uL ligation sample to 25 uL of competent cells and place on ice for 30 min
  - a. Change proportionally if the ligation mixture is more than 10 uL
7. Shock each tube in a 42-degree heat block for 45 seconds
8. Return to ice for 2 min
9. Add 1 mL of LB- make sure there are NO antibiotics in the media
10. Incubate at 37 degree for 30 min- 1 hr in the shaker
11. After incubation, centrifuge cells at 6000 rpm for 1 min
12. Remove 800-900 uL of supernatant and discard (leave a little bit in tube)
13. Resuspend cells in remaining supernatant by pipetting mixture in and out of pipette (10 or 100 uL pipette tip should be fine)
14. Transfer mixture to an ampicillin plate and spread solution on plate using end of a clear pipette
  - a. Spread on TOP of ampicillin then shake gently
15. After plate is dry enough, invert and incubate overnight at 37 degree C
  - a. Make sure to label plate with vector and date! Ex: PLNCX2-VenusC1-nsp5-D4  
3/2/22
16. After 24h, check for colonies to see if ligation is successful.

### **A.7 Colony PCR**

1. Fill microcentrifuge tube with 500 uL of LB + Amp
2. Grab a small pipette tip and with your hand and gently tap the top of the colony growing on the plate, being sure to not dig into the agar

3. Stir the tube containing LB with the tip
4. Incubate tube in shaker for 2-3 hours
5. During the incubation period, set up the EconoTaq PCR:
  - a. Note: The forward primer is usually designed from the gene of plasmid vector, and the reverse primer is designed from the gene of the template DNA

Reaction system table:

	Volume
2X PCR EconoTaq	5 uL
Forward Primer (10 uM)	0.5 uL
Reverse Primer (10 uM)	0.5 uL
Template DNA	1 uL
Nuclease-free water	3 uL
Total Volume	10 uL

6. After incubation, add 1uL of the ligation mixture to the PCR mix
  - a. If you are running PCR on multiple colonies, then add 1 uL per PCR mixture tube
7. Run EconoTaq PCR
8. Run DNA gel (Appendix B.8)

## A.8 Running DNA Gel (Using Quality One App for analysis)

1. Cut DNA gel w/ razor
  - a. You'll need one well for each sample plus one well for the ladder
  - b. Cut in the middle of the next well
    - i. If you need 5 wells for your sample plus ladder, cut in the middle of the sixth well
2. Add Running Buffer (1X TAE) to gel machine if necessary- enough to submerge gel
3. Add gel to to running buffer
4. Load DNA gel
  - a. Mix 2uL of sample with 2uL of loading buffer on Saran wrap and transfer mixture to well
  - b. Add 2uL of ladder
5. Run gel at 100-150V until the bands are about halfway down the gel (should be about 15 min)
6. Put gel in scanning machine
7. Open Quantity One app on computer (red emblem)
8. Move lever at top of scanning machine from O setting to I setting (in the middle)
9. Press Trans UV button on scanning machine
10. Click select scanner on computer and then select the only option that appears
11. Click live/focus to view gel
  - a. Transformation allows you to adjust contrast to see the faint bands
12. Click manual exposure to save
13. Throw out gel

## **A.9 Miniprep**

### **A.9.1 Inoculation for Miniprep**

1. Add 4 mL of LB + amp to a 14 mL culture tube
  - a. LB + amp should be 1:1000 amp:lb
2. Add 200 uL of bacteria sample to tube (colony PCR bacterial colonies- from appendix B.7)
3. Put in shaker overnight

### **A.9.2 Running Miniprep (Using GeneJET PCR purification kit)**

The purpose of this experiment is to extract a small amount of DNA that can be subsequently sequenced (using appendix A.4). This will allow us to check if nsp5-D4 was correctly inserted into the plasmid.

1. Add 1 mL of bacteria (from the inoculation) to a 1.5 mL tube
2. Obtain miniprep kit (GeneJET PCR purification kit)
3. Centrifuge 1.5 mL tubes at 12,000g for 1 min
4. Discard supernatant- DO NOT touch the pellet
5. Add 200 uL of resuspension solution (solution I in miniprep kit) to 1.5 mL tube (200 uL per tube) and aspirate to resuspend pellet
  - a. To avoid bubbles, leave some liquid in the pipette while aspirating
  - b. Can also vortex to help mix
6. Add 400 uL of lysis solution (solution II in miniprep kit) and slowly invert the tube to mix
  - a. DO NOT mix too fast/ too harsh

7. Add 300 uL of neutralization solution (solution III in miniprep kit) and invert tube a couple times
8. Centrifuge at 12,000 rpm for 15 min
9. Transfer supernatant to ThermoScientific GeneJET spin column (clear blue tube in miniprep kit)
  - a. Discard old microcentrifuge tubes
10. Centrifuge for 1 min at 12,000 rpm
11. Discard flow through
12. Add 700 uL of wash solution
  - a. Be careful with this step- add directly onto filter
13. Repeat steps 10 & 11
14. Repeat step 12, then repeat step 13
15. Centrifuge empty column for 2 min at 12,000 rpm
16. Move blue tube to a new 1.5 mL tube and add 50 uL of ddH<sub>2</sub>O to blue tube, incubate for 2 min
17. Centrifuge for 2 min at 12,000 rpm, then remove and discard blue tube
18. Store and label 1.5 mL tube containing plasmid in 4 degree fridge (next step is sequencing)
  - a. Label with vector, date, and concentration after you take the concentration (refer to Appendix A.3)

## **A.10 Midiprep**

### **A.10.1 Inoculation for Midiprep**

1. Add 100 mL of LB + amp to each 125 ml flask (same amp:lb ratio as miniprep)
2. Add 50 uL of bacteria (from glycerol stock or 14 mL culture tube used during miniprep)
  - a. If it is from glycerol stock, make sure to thaw bacteria ONLY slightly- do not let it thaw fully
3. Put in shaker overnight

### **A.10.2 Running Midiprep (PureYield Plasmid Midiprep System)**

The purpose of this experiment is to extract plasmid DNA that can be used in subsequent transfections, which will allow nsp5-D4 to be packaged into a delivery system that will allow it to enter lymphoma cells. The delivery system are retroviruses, which will be packaged in GP2-293 cells through transfecting the plasmid DNA into these cells. Midiprep allows us to have an adequate amount of DNA for this procedure (appendix B). The volumes of each solution added depend on the bacterial culture volume.

#### Preparing lysate

1. Take the flask out of the shaker and add 50 mL to two midiprep tubes (so 100 mL total transfer)
2. Pellet cells at 5,000 x g for 10 minutes.
3. Remove supernatant
4. Suspend pellet in 3 mL cell resuspension solution (invert 5-6 times).

- a. This is the most important step in the whole procedure. After decanting the supernatant, resuspend the pellet *vigorously* (perhaps with a 1 mL micropipette) until the fluid is a homogenous milky color. There should be no pellet left AT ALL.
  - b. Success in this step can be verified later: before the second centrifugation, the tube should have floating material that looks like shaved coconuts.
5. Add 3 mL cell lysis solution- invert 3-5 times to mix.
  6. Incubate 3 min at room temperature
  7. Add 5 mL neutralization solution. Invert 5-10 times to mix.
  8. Centrifuge lysate at 15,000 x g at room temperature for 15 minutes.

#### DNA purification

9. Assemble a column stack by placing blue PureYield Clearing column on top of white PureYield Binding Column. Place the column stack on the vacuum manifold.
10. Carefully pour supernatant into the column stack. Apply vacuum, continuing until all liquid has passed through both the clearing and binding columns.
11. Slowly release the vacuum from the filtration device. Remove the blue clearing column, leaving the binding column on the manifold.
  - a. Note: if the binding membrane has been dislodged from the bottom of the column, tap it back in place using a sterile pipette tip
12. Begin washing procedure by adding 5.0 mL of Endotoxin removal wash to the binding column, and allow vacuum to pull solution through the binding column.

13. Add 20 mL of column wash solution to the binding column, and allow vacuum to pull solution through the binding column.
14. Dry the membrane by applying the vacuum for 30-60 seconds. Repeat if the tops of the DNA binding membranes appear wet or there is a detectable ethanol odor.
15. Let the binding buffer dry (keep vacuum on) until cracks appear on the fabric. Then, turn off the vacuum, remove the binding column from the vacuum manifold, and dry off the bottom of the binding column with a kimwipe.

Elute by Vacuum

16. Place a 1.5 mL microcentrifuge tube at the base of the Eluator Vacuum Elution Device (Cat. #A1071), securing the tube cap.
17. Assemble the Eluator Vacuum Elution device and insert DNA binding column into the device, making sure that the column is fully seated on the collar.
18. Place the elution device assembly, including the binding column, onto the vacuum manifold.
19. Add 400-600 uL of Nuclease-free water to the DNA binding membrane in the binding column. Wait for 1 minute.
20. Label the 1.5 mL tube with the name of the DNA collected. Measure the concentration of the resultant DNA (appendix A.3) and then label the concentration on the tube.

## **Appendix B: Retroviral Packaging and Delivery through Transfection**

The protocol describes the basic steps for preparing a retroviral delivery system. The major parts include making the recombinant plasmid with the gene of interest inside the transfer

vector, cotransfecting the packaging cell line with the envelope plasmid and retroviral plasmid, and determining the retroviral titer.

**B.1 Recombinant Plasmid**

In order to insert the nsp5 gene into the pLNCX2 vector with the Venus tag, PCR and restriction enzyme cloning must be used. Refer to Appendix A for details.

**B.2 Packaging Retroviral Vectors**

Timeline	Steps
Day 0	Seed cells to be 90-100% confluent at transfection
Day 1	Dilute DNA/VSVG mixture with transfection buffer, then vortex 1 second and spin down
	Add certain ratio of transfection reagent, vortex 1 second, spin down
	Incubate at room temperature for 20 min
	Add transfection mix to cells in serum containing media
	Switch media after 4h
Day 2	Check 24h fluorescence
Day 3	Check 48h fluorescence
	Harvest cells

Procedure Details (per well)		
Component	24-well	6-well
Total well volume	0.5 mL	2 mL
Adherent cells	$0.4-1 \times 10^5$	$1.5-4 \times 10^5$
DNA	0.25 $\mu$ g	1 $\mu$ g
VSVG	0.25 $\mu$ g	1 $\mu$ g
jetOptimus Buffer	50 $\mu$ L	200 $\mu$ L
jetOptimus Reagent	0.75 $\mu$ L	2-3 $\mu$ L
Incubate for 20 min at room temperature.		
Add transfection mixture to one well of cells.		
Incubate cells for 48h at 37 °C and analyze.		

### B.3 Harvesting the Retroviruses from GP2-293 cells

After transfection occurs, the next step involves harvesting the retroviruses from the GP2-293 cells.

1. For every well plate harvested, gather 2 microcentrifuge tubes: 1 for supernatant and one for the pellet.
2. Aspirate the fluid in the cell with the supernatant in order to detach the cells from the bottom of the well.
3. Pipette the solution from the well into the pellet labeled microcentrifuge tube.
4. Centrifuge at 1000 rpm for 1 min.

5. Then, remove as much of the supernatant as possible and move this solution into the supernatant microcentrifuge tubes.
6. Freeze supernatant tube in the -80°C freezer.
7. Add 100µl of PBS and 100µl of Laemmli buffer into the pellet tube.
8. Boil the pellet tube in 100°C heat block for 10 min.
9. Cool on ice for 5 minutes.
10. Centrifuge at 12000 rpm for 5 minutes.
11. Store pellets in -20°C freezer.

#### **B.4 Determining Retroviral Titer by qRT-PCR**

*Protocol from Takara Bio USA.*

The titer of the harvested retroviral stock can be quantified in order to ensure an adequate amount is used for transduction (Appendix C). This is performed so that the transduction results can be properly interpreted. This will also verify the viability of the virus stocks. Titrations are used to meet this requirement. The method that will be used is qRT-PCR, or reverse transcription and quantitative PCR. Here, RNA transcripts collected from the previous step are quantified by initially reverse transcribing them into cDNA. Then, qPCR is carried out to assess amplification. The retro-X qRT-PCR titration kit accomplishes the titration in a 1 step, 4 hour protocol. This process is useful for freshly harvested viral stocks: it has been documented that a freeze-thaw cycle can significantly reduce retroviral titer. The following procedure is from the [Takara Bio USA Retro-X qRT-PCR Titration kit User Manual](#).

##### **B.4.1 Protocol Overview**

Viral supernatant is collected from your virus-producing cell line and centrifuged to remove cells and debris.

1. Using the NucleoSpin RNA Virus kit, genomic viral RNA is purified from a small aliquot of the supernatant.
2. The RNA is then treated with DNase I to remove any residual plasmid DNA that may have been carried over from transient transfection of the packaging cells.
3. Serial dilutions of the viral RNA sample are subjected to qRT-PCR to determine threshold cycle (Ct) values for each dilution.
4. Titration by qRT-PCR is also compatible with the ROX qPCR reference dyes provided with the kit (optional).
5. The RNA genome copy number in a sample dilution is determined by finding the copy number that corresponds to its Ct value on a standard curve generated from serial dilutions of the calibrated Retro-X RNA Control Template.

#### **B.4.2 Purifying Retroviral Genomic RNA**

\*Note: Clean work station- need to make sure there is no contamination (PCR room)

1. Harvest retroviral supernatant from transfected GP2-293 cells (using harvesting protocol)
2. Aliquot 200 uL of supernatant for immediate titration, or store in -80 degree fridge
  - a. Label tube with purpose (for retroviral titer procedure), date, vector
3. Purify RNA using the NucleoSpin RNA Virus Kit according to the protocols contained in [the NucleoSpin RNA Virus & Virus F User Manual](#) (pg 14- section 5.1). Smaller volumes (5–100 µl) can also be used if necessary.
  - a. Kit is located above our workbench
4. Elute RNA in 50-100 uL nuclease free water (in column used above- similar to our PCR product purification protocol)
5. Treat viral RNA samples with DNase I reaction:

a.

<b>Reagent</b>	<b>Volume (uL)</b>
RNA sample	12.5
DNase I Buffer (10X)	2.5
DNase I (5 units/uL)	4.0
RNase-Free Water	6.0
<b>Total</b>	<b>25.0</b>

- b. Combine reagents, mix, and incubate at 37°C x 30 min, followed by 70°C x 5 min. A thermocycler should be used for this reaction. Store the tubes on ice until ready to perform qRT-PCR.

#### **B.4.3 qRT-PCR amplification (PCR room)**

6. Assemble the following Master Reaction Mix (MRM) using the following reagents (add RT enzyme mix last). Depending on the number of RNA samples you have, this will change the overall amount of MRM you make. Use this table as a guide. Each well in the 96-well plate used for qRT-PCR needs 23.0 uL.

a.

<b>Reagent</b>	<b>Volume/well (uL)</b>
RNase-Free Water	8.0
Quant-X Buffer (2X)	12.5
Retro-X Fwd Primer	0.5
Retro-X Reverse Primer	0.5

ROX LMP dye	0.5
Quant-X Enzyme	0.5
RT Enzyme Mix	0.5
<b>Total</b>	<b>23.0</b>

b. Example Calculation for an experiment in triplicate

$$1 \text{ RNA sample} \times \frac{4 \text{ PCR tubes (for serial dilution)}}{1 \text{ sample}} \times \frac{3 \text{ wells in 96 - well plate}}{1 \text{ PCR tube}}$$

$$= 8 \text{ wells in plate per sample}$$

$$1 \text{ RNA control} \times \frac{8 \text{ PCR tubes (for serial dilution)}}{1 \text{ control}} \times \frac{3 \text{ wells in 96 - well plate}}{1 \text{ PCR tube}}$$

$$= 24 \text{ wells in plate per sample}$$

$$24 + 8 = 32 \text{ wells total}$$

$$32 \text{ wells} \times \frac{23 \text{ uL mastermix}}{1 \text{ well}} = 736 \text{ uL total}$$

- c. Add 10% to the total Mastermix (736 x 1.1) to account for any loss. Then, scale each individual amount to the new total using the table above.
- d. Create Mastermix in a 1.5 or 2 mL microcentrifuge tube.
7. Using PCR grade 8 well strips, construct a standard curve of Retro-X RNA Control Template dilutions, and make serial dilutions of your purified viral RNA sample(s) as described below and shown below:
- Each control, no template control (NTC) and sample reaction should be performed in triplicate
  - Assemble the serial dilutions in a qPCR reaction assembly area

- c. Note: one sample uses four PCR tubes. This protocol is showing preparation of 8 PCR tubes for two RNA samples in strip 1. Using the example above (when we created mastermix), only tubes 1-4 in strip 1 would be used.

### Control and Sample Dilutions for qRT-PCR

(2 uL of each will be used for each qRT-PCR reaction)

	<b>Strip 1: Samples</b>		
<b>Well</b>	<b>EASY buffer</b>	<b>Additive (uL)</b>	<b>Amount (copies/uL)</b>
<b>1</b>	-	20	Sample 1: 1X
<b>2</b>	27	3	0.1X
<b>3</b>	27	3	0.01X
<b>4</b>	27	3	0.001X
<b>5</b>	-	20	Sample 2: 1X
<b>6</b>	27	3	0.1X
<b>7</b>	27	3	0.01X
<b>8</b>	27	3	0.001X

	<b>Strip 2: Controls</b>		
<b>Well</b>	<b>EASY buffer</b>	<b>Additive (uL)</b>	<b>Amount (copies/uL)</b>
<b>1</b>	18	2	$5 \times 10^7$
<b>2</b>	27	3	$5 \times 10^6$
<b>3</b>	27	3	$5 \times 10^5$
<b>4</b>	27	3	$5 \times 10^4$

<b>5</b>	27	3	$5 \times 10^3$
<b>6</b>	10	-	NTC
<b>7</b>	10	-	NTC
<b>8</b>	10	-	NTC

Set up as individual PCR reaction tubes:

<b>Strip 1: Samples</b>							
1	2	3	4	5	6	7	8
<b>Strip 2: Controls</b>							
1	2	3	4	5	6	7	8

8. Add EASY Dilution Buffer to the appropriate wells of the strips, as shown in the table above. NTCs in Wells 6–8 of Strip 2 contain only EASY Dilution Buffer.
9. In Wells 1–5 of Strip 2, prepare 10-fold serial dilutions of the Retro-X RNA Control Template as follows:
  - a. In Well 1, dilute 2  $\mu$ l of the Retro-X RNA Control Template stock into 18  $\mu$ l of buffer for a 1:10 dilution (10X stock =  $5 \times 10^8$  copies/ $\mu$ l).
  - b. In Wells 2–5, perform 10-fold serial dilutions of the diluted control template in Well 1 by transferring 3  $\mu$ l of Well 1 into the 27  $\mu$ l of buffer in Well 2. Repeat similar dilutions for Wells 3–5.
10. Serially dilute your viral RNA samples as shown in the table above (strip 1). Each 8-well strip can be used for 2 samples at 4 different concentrations each.
  - a. The first well in each series (Wells 1 & 5) should contain 20  $\mu$ l of undiluted sample (1X).

- b. Subsequent 10-fold sample dilutions (Wells 2–4 & Wells 6–8) can be made by serially transferring 3  $\mu$ l of the preceding dilution into 27  $\mu$ l of buffer in the next well.
11. Mix well by tapping gently and centrifuge the strips at 2,000 rpm (4°C) for 1 min to remove any bubbles.
  12. Place a 96-well PCR plate on ice and dispense 23  $\mu$ l/well of MRM into the appropriate wells (in triplicate) using a repeating pipet
  13. Using a multichannel pipet, transfer 2  $\mu$ l/well of the control dilutions, NTCs, and sample dilutions (in triplicate) from the 8-well PCR strips to the PCR plate containing MRM.
  14. Centrifuge the plate at 2,000 rpm (4°C) for 2 min to remove any bubbles.
  15. Program your real-time qPCR instrument for the following qRT-PCR reaction cycles. Include a final dissociation curve cycle. Install the plate in the instrument and start the program:

<b>RT Reaction</b>	
42 °C	5 min
95 °C	10 sec
<b>qPCR x 40 cycles</b>	
95 °C	5 sec
60 °C	30 sec
<b>Dissociation Curve</b>	
95 °C	15 sec
60 °C	30 sec

All (60 °C- 95 °C)	
--------------------	--

16. After the run is complete, look at the average Ct values and copy numbers to calculate the copy number/microliter in each sample. This can then be used to determine the amount of RNA needed for the transduction protocol, in Appendix C.

### **Appendix C: Transduction of target gene into Lymphoma cell line**

This protocol will describe the transduction procedure that was used to insert the retroviruses containing nsp5 made from the packing cell line, GP2-293, into a lymphoma cell line, BCBL-1 (refer to Appendix B for transfection details). The purpose of this protocol is to express nsp5 in lymphoma cells to assess if STAT3 is successfully downregulated in cancer cells. Cancer cells have an upregulated STAT3 pathway that allows for uncontrollable cell proliferation. D4 in nsp5 is expressed in the BCBL-1 cancerline and further assessed for upregulated cell proliferation.

#### **C.1 Delivery of packaged retroviruses into BCBL-1 cell line**

Once the recombinant retrovirus was isolated from the GP2-293 cell transfection, a transduction was performed on BCBL-1 cells to deliver nsp5 to lymphoma cells. The supernatant isolated was concentrated using Retro-X™ Concentrator (Takara Bio). After concentration, the supernatant was added to the BCBL-1 cells on a well plate with media. In addition, polybrene was added to increase transduction efficiency. The cells were left to incubate for a maximum of 72h, with checkpoints for fluorescence at 24h, 48h, and 72h using the fluorescence microscope. Additionally, cell counting was done at the same checkpoints to monitor cell health and density. Fluorescent cells indicate the successful

transduction of nsp5 into BCBL-1 cells and its subsequent gene expression and protein production.

Timeline	Steps
Day 0	Cells in the flask should be 90-100% confluent.
	Harvest supernatant from transfection and concentrate using the Retro-X™ Concentrator.
Day 1	Take supernatant with Retro-X™ Concentrator and centrifuge at 14,000 rpm for 5 min
	Add media to well plate and gently swirl
	Add cells to well plate and gently swirl
	Add polybrene to well plate and gently swirl
	Pipette to mix supernatant
	Add concentrated supernatant to well plate
Day 2	Check 24h fluorescence and count cells
	Check 48h fluorescence and count cells
Day 3	Check 72h fluorescence and count cells
	Harvest cells

Procedure Details (per well)		
Component	24-well	6-well

Suspension cell #	2.5x10 <sup>5</sup>	5x10 <sup>5</sup>
Polybrene	1.25 µl	1.8 µl
Supernatant	.75 ml	1 ml
Media	100 µl	100µl
Gently swirl the well plate to mix.		
Incubate cells for 72h at 37°C and harvest.		

### C.2 Harvesting BCBL-1 Cells for Analysis on Gene Expression

Harvesting BCBL-1 cells is done at the 72 h post-transduction point for analysis of STAT3 expression in the presence of viral protein nsp5. The procedure to harvest BCBL-1 cells is outlined below. After completing this, the next step is to analyze the expression of nsp5 and its effects on STAT3 in this lymphoma cell line via analysis of tumor cell regression through Western Blot (WB) analysis, with an empty vector used as control, a cell viability assay, and a reporter assay (see Appendices E, F and G for more information).

1. Add all of the of BCBL-1 cells to the appropriate tube
2. Centrifuge for 5 min at 1000 rpm to pellet cells
3. Discard supernatant
4. Resuspend pellet in 30 uL of PBS
5. Add 20 uL of Laemmli buffer to each tube
6. Freeze at -20 degrees celsius

## **Appendix D: Cell Culture and Maintenance**

### **D.1 Subculturing Mammalian Cells**

*Protocol adapted from ThermoFisher Scientific*

This protocol describes the general procedure for subculturing mammalian cells in culture. Subculturing is the removal of medium and transfer of cells from a previous culture into a fresh growth medium, which enables further propagation of the cell line.

This can be important when there is a high cell density, or when there is an exhaustion of the medium, which prevents cell growth.

#### **D.1.1 GP2-293 Cells (Adherent)**

1. Check to ensure GP2-293 cells are 90-100% confluent
2. Warm up media (DMEM + FBE)
3. Remove and discard the spent cell culture media from the culture vessel.
4. Wash cells using a PBS (approximately 2 mL per 10 cm<sup>2</sup> culture surface area).

Gently add wash solution to the side of the vessel opposite to the attached cell layer to avoid disturbing the cell layer, and rock the vessel back and forth several times. Repeat 2X.

- a. The wash step removes any traces of serum, calcium, and magnesium that would inhibit the action of the dissociation reagent.
5. Remove and discard the PBS from the culture vessel
6. Add trypsin to the side of the flask; use enough reagent to cover the cell layer (approximately 0.5 mL per 10 cm<sup>2</sup>). Gently rock the container to get complete coverage of the cell layer.

7. Incubate the culture vessel at 37 °C for approximately 3 minutes.
8. Observe the cells under the microscope for detachment.  
  
When  $\geq 90\%$  of the cells have detached, tilt the vessel for a minimal length of time to allow the cells to drain. Add the equivalent of 2 volumes (twice the volume used for the dissociation reagent) of pre-warmed complete growth medium. Disperse the medium by pipetting over the cell layer surface several times.
9. Transfer the cells to a 15-mL conical tube and centrifuge them at  $800 \times g$  for 5 minutes.
10. Resuspend the cell pellet in a minimal volume of pre-warmed complete growth medium
11. Dilute cell suspension for appropriate amount of splitting, and pipet the appropriate volume into new cell culture vessels with vented caps, and return the cells to the incubator.
  - a. For 1:2 splitting, add 2 mL of DMEM + FBE
  - b. For 1:3 splitting, add 3 mL of DMEM + FBE
  - c. Aspirate to get cells to be single-celled. Check under a microscope to see if most cells are single-celled.
12. Spray + clean station
13. Add bleach to the liquid waste container to deactivate microorganisms
14. Close the hood, and turn on the UV light

### **D.1.2 BCBL-1 Cells (Suspension)**

Subculturing suspension cells is somewhat less complicated than passaging adherent cells. Cells are already suspended in growth medium, so there is no need to treat them enzymatically to detach them from the surface of the culture vessel, and the whole process is faster and less traumatic for the cells. Replacement of growth medium is not carried out in suspension cultures; instead, the cells are maintained by feeding them every 2 to 3 days until they reach confluency (when cells clump together).

1. Warm up media (RPMI + FBE)
2. Remove appropriate mL of cells from flask (4 mL for T25 flask)
3. Add 3-4 mL of media to flask
4. Store in CO<sub>2</sub> incubator
5. Spray + clean station
6. Add bleach (by the sink) to the liquid waste container to deactivate microorganisms
7. Close the hood, and turn on the UV light

### **Appendix E: Equity Impact**

This research project aims to study a more targeted and less invasive method to cancer treatment by using viral protein nsp5 to target the STAT3 pathway in lymphoma cancer cells. This would potentially be a way to induce tumor cell death without causing too much damage to normal cells. Current treatments such as surgery, chemotherapy, and radiation can be invasive because of incisions on the body, and by giving the body high doses of drugs and radiation that cause harm not only to cancer cells but also to normal cells. This leads to the negative side effects that we see with cancer treatment such as physical and emotional pain. The team is

hoping to contribute to the body of knowledge so that the information on the use of viral protein nsp5 can be used by others to develop more efficient and less harmful cancer treatments for clinical applications. The costs of such treatments can be lowered by motivating federal funding and programs to help support individuals who need treatment. In addition, such treatments can reduce side effects and the time spent in the hospital. This can have multiple implications. First, it would save the cost of additional medications and extended hospital stays. It would also allow individuals to recover quicker so that they can return to their work sooner. Therefore, such treatment would be beneficial to low-income and minority individuals who often have these concerns. Additionally, the less stress related to cost can help with their psychological well-being which is important to better treatment prognosis.

Another benefit of this research is the diverse perspectives that it provides. Cancer research often lacks diverse views, especially from minority individuals. This is due to both not having enough research on how cancer impacts minority groups and not having diverse researchers running the research. This research project is being conducted by a diverse group of individuals, each with different backgrounds and views. Therefore, the research takes into account a wide range of audiences and target groups for cancer treatment. It also takes into account the cultural, social, and economical considerations that are important when treating diverse patient populations, especially when working with racial and ethnic minority groups. In addition to the impact it would have on the target groups for the cancer treatment, the research will also contribute to diverse perspectives in literature. Such perspectives can be used in the future to better design basic cancer research and clinical trials. As a result, research studies will be able to translate to larger and more diverse populations.

This research is one of the first steps leading to drug development and clinical trials. As such, it is important to consider how our research can be used in the future, should it progress to *in vivo* models and continue into drug development. One aspect to consider is the cost of drug development. After medicine goes through clinical trials, treatments are often really expensive if the disease is rare, because pharmaceutical companies need to make a profit. Therefore, to make an equitable treatment, we need to look into how we can reduce drug development costs. Additionally, we would need to consider alternative options and insurance so people of diverse backgrounds can get the medicine they need should the treatment be successful. That is why developing a cancer treatment that can be applied to a wide variety of cancers is appealing- it would allow a drug to reach a wider audience, and make it more attractive to spend the time, money, and energy on for drug development. Since STAT3 affects a wide variety of cancers, if a treatment for this pathway advances into clinical trials, it may result in reduced prices in the long run. This is because patients may not need to spend money on extensive follow-ups or repeated applications of chemotherapy. It would also allow people of diverse backgrounds to access the treatment.

If the nsp5 treatment for STAT3 is successful *in vitro* and undergoes *in vivo* modeling, it may also be beneficial to test this treatment in combination therapies with current chemotherapy drugs. That way, we can assess if there are ways to make the treatment stronger and more appealing to study in clinical trials. This could create more incentive to develop the drug, and use it for personalized medicine- treatment based on a patient's genetics, drug tolerance, environment, etc.

### **Appendix E.1: Equity-Centered Design Model**

The aspects of equity-centered research discussed above can be applied to the Equity-Centered Community Design model created by Creative Reaction Lab. This is a unique creative problem-solving process based on equity, humility-building, integrating history and healing practices, addressing power dynamics, and co-creating with the community. This design process focuses on a community's culture and needs so that they can gain tools to dismantle systemic oppression and create a future with equity for all. This model brings together all different sects of people, such as researchers, designers, collaborators, and policy and business experts. Although the scope of our project will unlikely reach the phase of clinical testing and working with communities, it is still essential to consider the future directions.

The first step of the model is inviting diverse co-creators. Our project initially started with consulting our mentor and librarian, and then financial donors through crowdfunding. We also consulted various employers, professors, and previous lab members in the biomedical field for advice on cell maintenance. The next two steps are building humility and empathy and defining and assessing community needs. In order to build humility and empathy, we considered the perspective of the people we are trying to treat by developing specialized cancer treatment. In order to assess community needs, we would look at the impact that lymphoma has on the community and the patients who suffer from the disease. Additionally, other steps include history and healing and acknowledging and dismantling power constructs. This research aims to find a less invasive and more targeted treatment for lymphoma, which is aimed to be accessible to the public, especially minority populations. We would look into past treatments and expenses to inform our decisions. We want to ensure that our project does not develop into a treatment that is only available to nonminorities and the wealthy.

The sixth step is ideating approaches. The initial approach our team took was looking at nsp5's effect on the STAT3 degradation pathway *in vitro* by transducing lymphoma cells. If we had more time to successfully show tumor reduction, we could then consider *in vivo* models, which could ultimately lead to the clinical stage. The last two steps, rapid prototyping and testing and learning, can be applied to various stages of developing a cancer treatment. The ultimate goal would be to develop an anticancer therapeutics using nsp5. Therefore, it is essential to take the time to ensure accurate results of each stage before, during, and after drug development. That way, we can ensure that this treatment would be safe, efficient, and equitable.